SISSA - SCUOLA
INTERNAZIONALE
SUPERIORE
DI STUDI AVANZATI
TRIESTE
Strada Costiera 11

ISAS - INTERNATIONAL SCHOOL FOR ADVANCED STUDIES

Thesis submitted for the degree

of

"MAGISTER PHILOSOPHIAE"

"AU (111) SURFACE RECONSTRUCTION"

Candidate

Anna Bartolini

Supervisor

Prof. Erio Tosatti

Academic Year 1985/86

TRIESTE

I N D E X

I would like to express my gratitude to Prof. E. Tosatti who has given me the ideas for this work, during very useful discussions.

I owe Doct. F. Ercolessi particular thanks. In fact he followed me very patiently during the work at the computer, explaining to me his programs and the way to use them. He helped me at the beginning also in the understanding the theory of surfaces.

I would also mention Doct. M. Garofalo and Doct. C. Z. Wang, who have illustrated to me some parts of their researches that were useful for my thesis.

INTRODUCTION

It has been known for many years that clean metals surfaces may reconstruct, that is, may have a structure that is not a simple termination of the bulk structure. One of the basic aims of surfaces science is just to investigate the geometric arrangement of atoms in the first few layers of a crystal; in fact other quantities, such as the surface density of states, the electronic work function, and chemical bonding or chemical reaction in the presence of adsorbates, are correlated to structure parameters.

The knowledge of the surface structure is of particular importance in studies of surface and bulk phase transitions, especially for the understanding of the mechanism of phase transitions, and to test theories proposed to explain their occurence.

The precise location of atoms in the reconstructed surface must also been known for the analysis of the electronic structure of the metal surface. Finally, the surface structure plays an important role in crystal growth and in epitaxy.

The first clean metals surfaces known to reconstruct are the (100) faces of Ir,Pt,Au,V,Cr,Mo,W, the (110) faces of Ir, Pt, Au and the (111)face of Au.

It can be seen that, among the noble metals, gold stands out just for its remarkable surface properties. In fact all low-

index surfaces reconstruct, in such a way to give rise to close-packed layers. Here we study in particular Au (111) face reconstruction.

After having described some experimental techniques used to investigate surface structures, we shall review the informations got from experimental studies of Au (111) surface and some models proposed to explain them. In detail we shall review a model in which the Au (111) reconstruction is explained by the presence of walls of solitons (cap. 1).

Then we shall introduce a new scheme, the "glue" model, by which it has been already possible to explain well the behaviour of Au (100) and Au (110) surface reconstructions. Particular attention will be given to the "glue" term added to a two-body term in the Hamiltonian used to describe the metal. Many examples can in fact illustrate the insufficiency of a two body term to explain a lot of physical properties, like electronic cohesion in metals or the behaviour of elastic constants.

We shall shortly review also a possible microscopic mechanism proposed by Heine and Marks, but without attempting a quantitative modeling. In fact at the "ab initio" microscopic level the task of describing surface reconstruction of gold is certainly a very difficult one. Therefore nowdays the only possibility of describing the properties of metal surfaces is to apply to phenomenological models.

In practice we shall use a phenomenological Hamiltonian by F. Ercolessi, M.Parrinello, E.Tosatti, including the many body force

term, the "glue", carefully optimized to account phenomenologically for a vast variety of properties of solid and liquid gold.

Another attempt of this kind has been done by M.I.Daw and M.S. Baskes,whose theory also will be shortly considered (cap.2).

The scope of this work is, within the already mentioned glue model, to obtain the optimal atomic configuration of Au (111) slabs at T=0 and to study their reconstruction at higher temperatures. The optimal atomic configuration of (111) slab is obtained by a molecular dynamics strategy. By varying cell size and atom number, the lowest energy configuration is found $11x2\sqrt{3}$ at T=0. We shall investigate also the presence of solitons and their modification, increasing temperature.

The reconstruction will be found to be very stable until high temperatures; we shall also check the temperature at which the reconstruction starts to disappear.

To see better the transition from a floating phase to a disordered one, the study of correlations among particles will be just started and our preliminary results will be reported, even if we cannot give at this point any final explanation for these (cap.3).

1) EXPERIMENTAL STUDIES OF AU (111) SURFACE RECONSTRUCTION AND MODELS PROPOSED TO EXPLAIN THEM.

Among the techniques sensitive to surface structure, there is diffraction of low energy particles with De Broglie wavelenghts of the order of the lattice constants,resulting from ionic scattering and atomic or molecular scattering. Methods more sensitive to local order, such as angular resolved photoemission spectroscopy or angular resolved Auger-electron spectroscopy (AES), are also in progress.

Low energy electron diffraction (LEED), however, is the oldest and most commonly method for surface structure determination. A more or less coherent beam of electrons in the energy range of about 20-600 ev, that is with wavelenghts between 3 Å and 0.5 Å, impinges on the crystalline surface. The elastically backscattered electrons, separated from an inelastic background by retarding fields grids,display the diffraction pattern of the surface on a luminescent screen. Both electron beam generation by an electron gun and detection of the diffraction pattern can be easily performed by commercially available UHV equipment.

Other techniques used are:

RHEED (Reflection high energy electron diffraction)

RBS (Rutherford backscattering)

TEM (Transmission electron microscopy)

TED (Transmission electron diffraction)

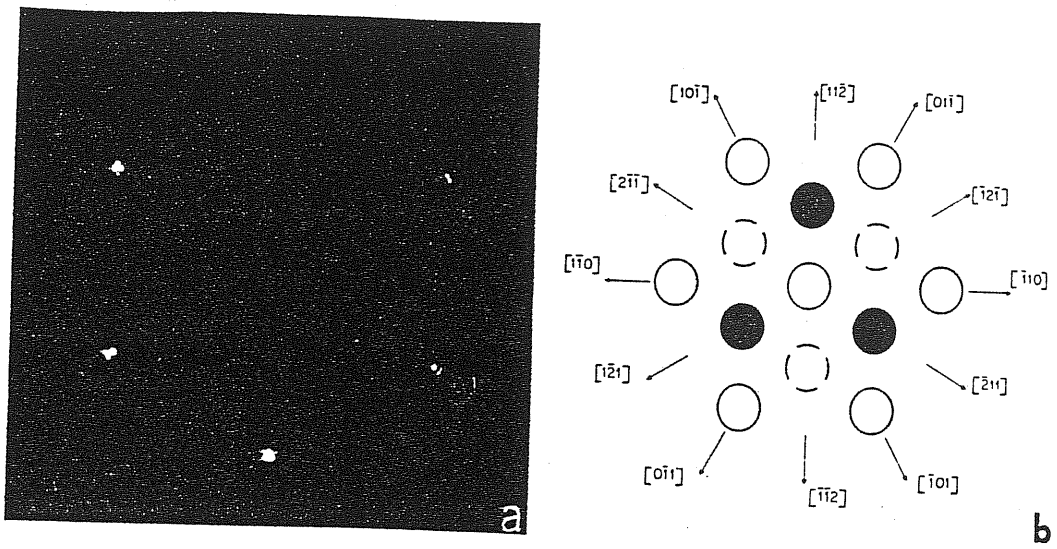

Fig. 1 a) LEED pattern at a primary beam energy of 54 eV from a clean Au(111) surface.
b) Orientation of sample with respect to LEED pattern. To be viewed from the prospective of looking through the crystal and projecting the first three layers, ABC, onto the screen, A = O, B = ○, C = ●.

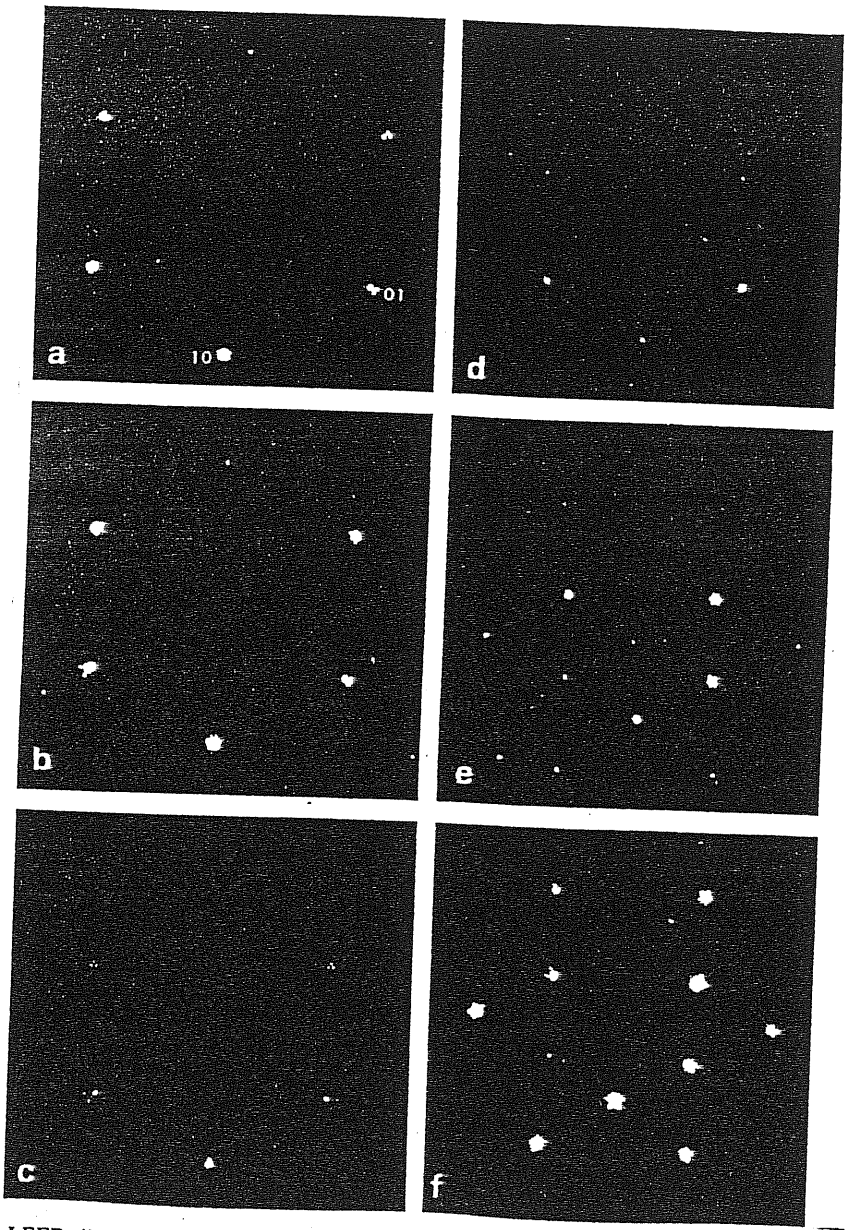

Fig. 2 LEED diffraction patterns for clean reconstructed Au(111) (courtesy of J.F. Wendelken and D.M. Zehner): (a) 46 V, (b) 54 V, (c) 64 V, (d) 80 V, (e) 133 V, (f) 145 V.

STM (Scanning tunneling microscopy)

Helium atom diffraction.

1.1 - Superstructures observed by LEED, RHEED, TEM and TED.

Concerning the surface reconstruction of gold (1,2), we know since earlier work by Fedak and Gjostein (3) that the gold surfaces (100) and (110) exhibit superstructures, respectively (5x1) and (2x1), but the (111) surface was generally described as an unreconstructed one (4-7). However published LEED photographs obtained during these studies, exhibit large areas of intensity at the integral order reflection positions instead of sharp narrow beams.

Then,in 1974, Perdereau et al. (8) have observed by LEED a superstructure on a (111) gold surface. According to these authors, the outermost layer looks like an hexagonal one, compressed by nearly 5% compared with the layer in the bulk.

Zehner and Wendelken (9), using the same technique ,have found that the geometry of the reordered layer is similar to that described by Perdereau et al. (8), but the compression is only 4% (figg. 1-2).

More recently, Melle and Menzel (10) have observed by RHEED a (pxl) with p=22-23 superstructure of the (111) face; in the (112) direction the outermost layer has the same parameter as the bulk, but in the perpendicular (110) direction, it is compressed by 4.2%. Therefore, the surface net has only a twofold symmetry instead of a sixfold one (figg.3-4).

As far as the fringes are concerned, Yagi et al.(11-12) have observed by UHV TEM periodic contrasts along the 3 (112) directions of the (111) surface of flat gold crystallites grown on MoS_2 and MgO substrates. Their spacing is about 63 Å. According to these authors, these fringes are the results of an unknown superstructure of the clean (111) gold surface.

J. C. Heyraud and J.J Metois (13) study flat gold crystallites with anomalous spots in TED and the fringes by Yagi et al.(11-12) in TEM. Their explanation for the two kinds of anomalies is based on the results obtained by Melle and Menzel concerning the superstructure(23x1) of the (111) gold surface.

Van Hove et al.(1-2) give a more complete interpretation of the LEED diffraction pattern observed by Wendelken and Zehner (8): three 120° rotated domains, each domains consisting of rectangular $(2\sqrt{3}\times\sqrt{3})$ cells. They notice that a model consisting of a 4.55% uniaxially contracted hexagonal top layer satisfies the observed diffraction pattern, the contraction direction being,as already said, a (110) direction. They interpret also the TEM results with fringes (not seen with other metals in (111) orientation) of about 63 Å periodicity with just the carachteristics expected from the model now described (fig.5).

Van Hove et al. (1-2) propose other two kinds of models. One is a domain structure model involving alternate strips 11 atoms wide of different bulk structure termination . An interesting possibility is

Fig. 3. RHEED diagram of Au(111)(23×1). Primary beam parallel [$11\bar{2}$].

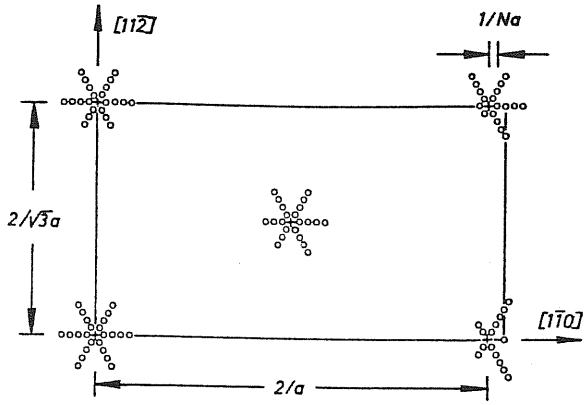

Fig. 4. (111) base of the reciprocal lattice for three supernets of Au(111)(23×1) extracted from patterns
. Crosses: foot points of rods corresponding to the ideal surface of bulk gold. Circles: the same corresponding to the beat frequencies.

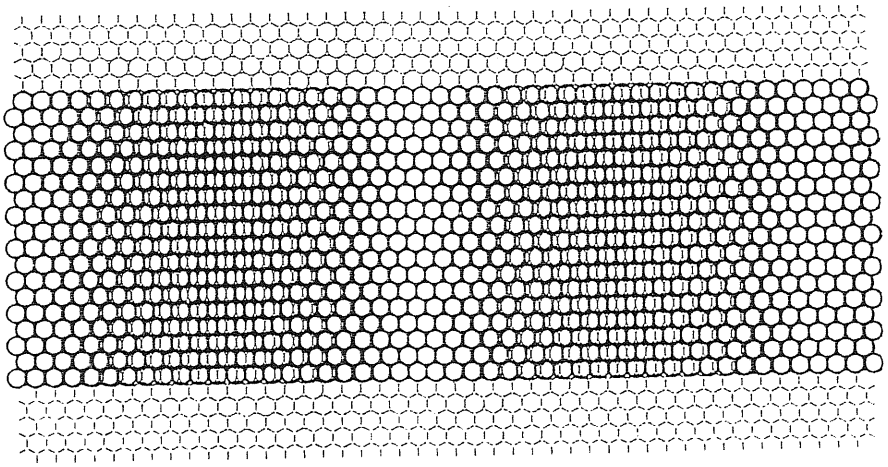

Au (111)(R3x22)rect

Fig. 5 Hexagonal model for Au(111)($\sqrt{3} \times 22$)rect reconstruction

that half the strips have the normal fcc termination, while in the other strips an hcp termination occurs through slippage of the topmost layer to different hollow sites of the second layer. For this model to be stable the two types of termination should have only a small difference in surface energies.

Another possibility, according to Van Hove et al.(1-2) for Au (111) reconstruction, is based on the concept of charge density wave. In fact, in general, some surface reconstructions, have been suggested to be caused by charge density waves in which the conduction electron density has periodic fluctuations with a wavelenght a few times the lattice constant, thereby inducing a static wavelike deviation of the atomic equilibrium position with that same wavelenght. For the Au (111) surface reconstruction, in particular, another possible model consists of charge density waves with an unusually long wavelenght of about 22 lattice constants.

It must be noticed that an approach to observe surfaces of monolayers levels by TEM had not attracted at the beginning much attention because of the following reasons: first,in the poor vacuum of an ordinary electron microscope, it was difficult to produce or mantain clear surfaces; secondly, image contrasts due to surface were thought to be overshadowed by strong scattering from the underlying bulk lattice. Instead, in the UHV electron microscope of Tanishiro et al.(14) thin Au platelets prepared by in situ deposition had clean surfaces and could

be kept uncontamined for a long time.

Y. Tanishiro et al.(14) have been the first who have studied the diffraction spots increasing temperature (figg.6-7). Their TEM and TED observations have led to the following scheme of the surface structure change: with increasing temperature the domains of the 6.3 nm spaced reconstructed surface structure become smaller and the unidirectional shrinkage of the surface layer transforms gradually to an isotropic, but a little bit smaller one, at high temperatures. At about 900 °C the reconstruction disappears.

Besides the confirm of one accord with the RHEED study by Melle and Menzel (10) and with the TEM study by Heyraud and Metois (13), the observations of Tanishiro et al.(14) have shown more directly the shrinkage and domain structure of the surface. Moreover, it was clearly demonstrated that the shrinkage of about 4% from the bulk Au (111) lattice takes place independently of the change of the underlying Au lattice parameter.

The more important evidence given by TEM is that the fringes are not simple interference fringes due to the shrunk surface and underlying lattice. The observation suggests the existence of some definite regions with structure strains like those of misfit dislocations.

The phase transition of the reconstructed Au surface was also noticed by Melle and Menzel (10) in their RHEED study.

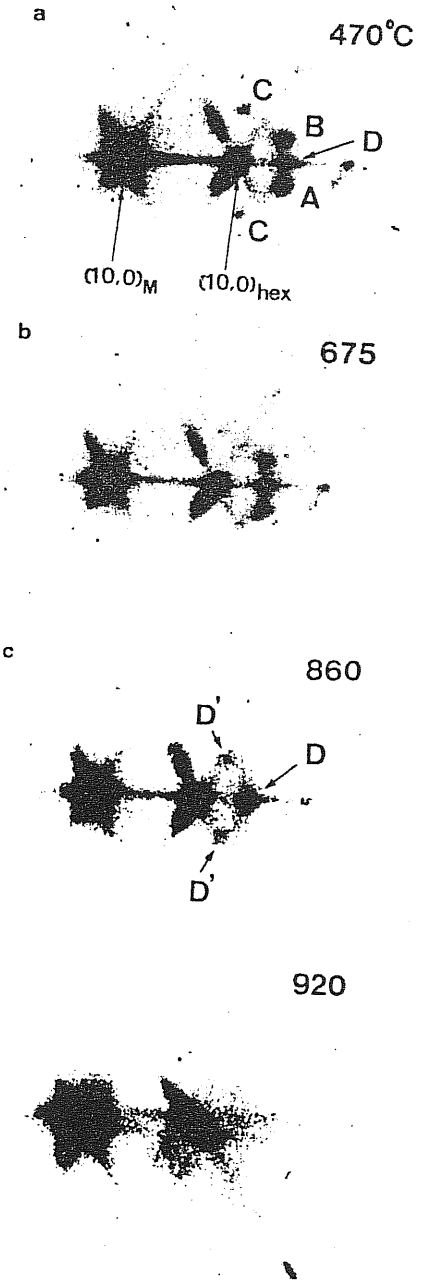

Fig. 6. Change of the surface structure diffraction spots at high temperatures. Note the disappearance of the spots A, B and C, the increase of the intensity of the spot D in (c), and the disappearance of the spots D and D′ in (d).

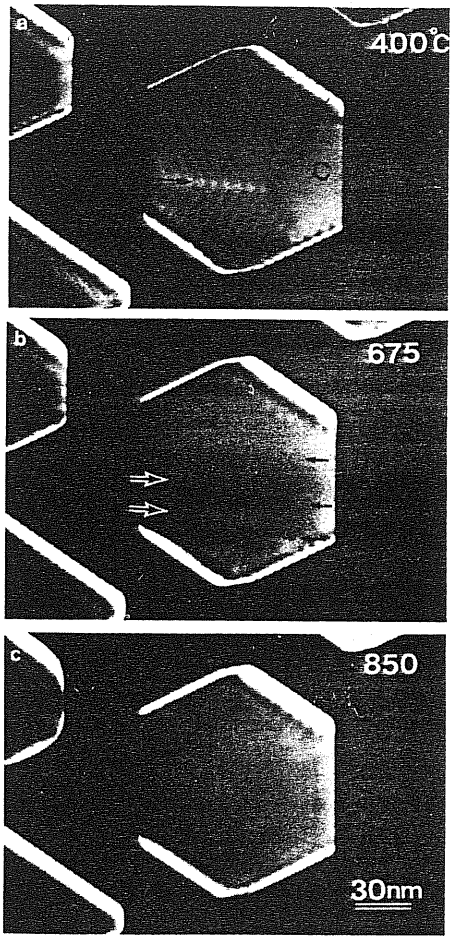

Fig. 7. Change of the surface structure image at high temperatures.

They observed a monotonic fading out of the extra spots into the background at elevated temperatures. The weakening of the fringes contrast at elevated temperatures above 500-600 °C has been also reported by Tanishiro (14). However, the observation of Tanishiro,as already noted, showed that, with increase of the temperature, the unidirectional shrinkage of the surface first layer transforms to an isotropic one, and finally the reconstruction disappears. The transformation is very gradual and takes place homogeneously on the surface.

More recent higly resolved TED experiments by Takanayagi and Yagi (15) suggest that the shrinkage along (100) direction is not uniform, but localized in two narrow transition regions where the stacking changes abruptly from ABC (fcc structure) to ABA (hcp structure) per unit supelattice cell, the transition region containing 0.5 atom each.

Anyhow, in contrast to these observations, Marks, Heine and Smith (16) have reported on electron microscopy studies which reveal an expansion of about 5% both normal to and within the surface plane.

This expansion will be shown to be in agreement with a strong repulsion between the d shells of the atoms resulting from depletion of sp electrons in the surface layer, according to the model proposed by Heine and Marks (17).

1.2 - Observation of a soliton reconstruction of Au (111) by helium atom diffraction.

U. Harten et al. (18) have studied Au (111) single crystal surfaces with high resolution helium atom diffraction. Compared to TED experiments He-atom diffraction probes only the first layer and is insensitive to the bulk. Their diffraction results show up to five satellites of the specular beam along the (110) direction with a particularly strong second order peak . They also notice a shift and a splitting of the (112) diffraction spots and threefold symmetry of the full diffraction pattern in place of the sixfold symmetry seen in many previous experiments (figg. 8-9).

Their observations are compatible with the already discussed model proposed for the reconstructed Au (111) surface (superlattice with a 22-23x$\sqrt{3}$ rectangular unit cell) involving an uniform compression of the surface layer in the (110) direction and also giving three possible domains.

U. Harten et al. (18) provide support for the new model, already discussed, proposed recently by Takayanagi and Yagi (15). But this model fails to explain the detailed intensity behaviour of the superlattice spots, or the exact positions of the components of the (112) peaks. Therefore, U. Harten et al. (18) propose a new model in which the reconstruction is characterized by the presence of solitons (appendix 1).

In particular, in their model, within C and A regions the atoms are at positions defined by bulk lattice spacing, i. e. , in registry with the second layer. The transition between C and A regions is described by a gradual x-dependent shift (x along (110)) given by the soliton expression (18) :

$$f(x) = 2/\pi \arctan\left(\exp \frac{x}{\Delta S}\right) \qquad (1)$$

where $2\Delta S$ is the half width of a soliton centered at the boundary A and C regions. In this model the transition region is larger than the narrow transition region by Takayanagi and Yagi (15).

In such a region, where the soliton causes a very gradual shift from the A to the C stacking, the atoms are raised up in the z direction by a x-dependent amount H(x) modeled by a Gaussian with height H and half width ΔS centered at the solitons (fig.10).

To test this model they have performed hard-wall eikonal calculation (27); the hard corrugated wall is defined by placing Gaussians at the surface layer atom positions, giving an effective peak to peak corrugation of amplitude h. With an appropriate choice of the parameters they obtain good comparison between experiments and results of calculations.

U. Harten et al. (18) write that if the soliton superlattice proposed in this model is correct, it may be indicative of the existence at the surface of two competing potential contributions of dif-

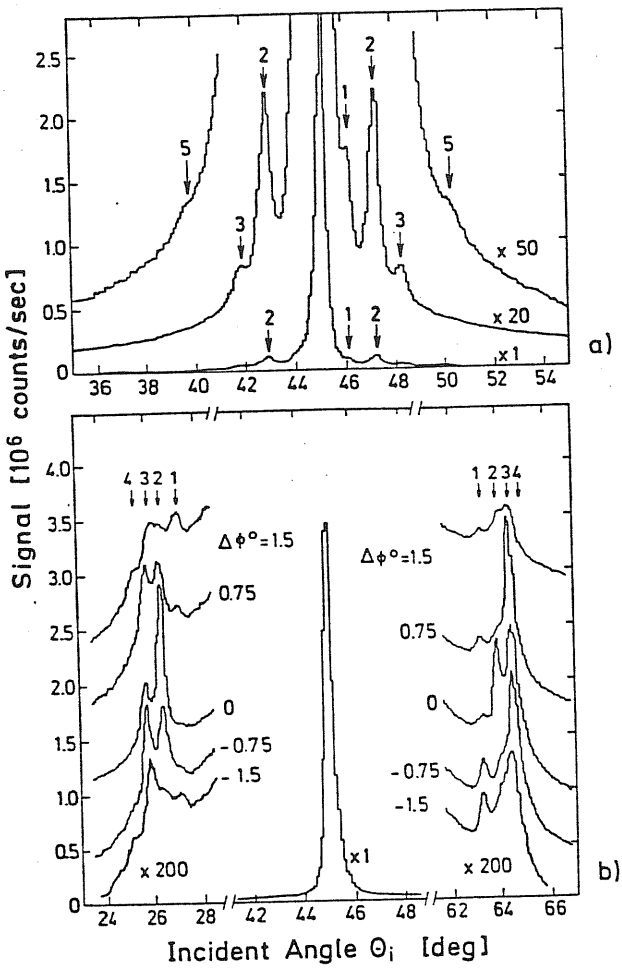

FIG. 8. He diffraction scans from the Au(111) surface. The crystal temperature was 300 K. (a) Along ⟨110⟩ at $k_i = 3.90$ Å^{-1} ($E = 7.95$ meV), (b) along ⟨112⟩ at $k_i = 5.64$ Å^{-1} ($E = 16.6$ meV).

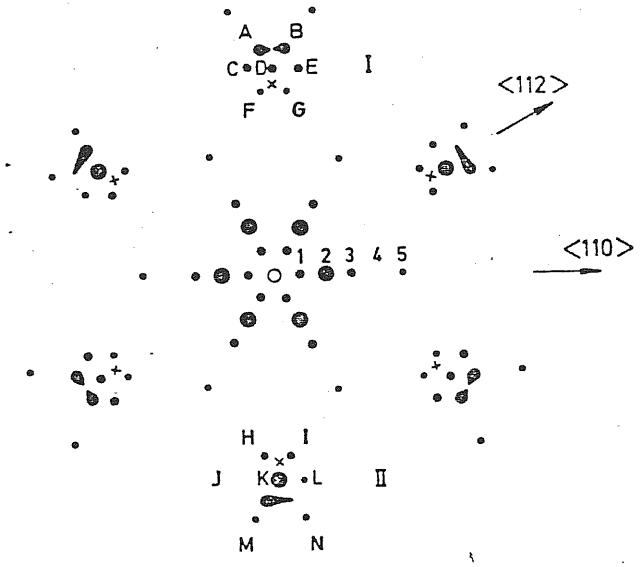

FIG. 9. Schematic representation of full diffraction pattern. The patterns in the ⟨112⟩ direction have been shifted towards the center, but otherwise the relative positions are to scale. (The spot size is proportional to intensity and magnified by a factor of 10 in the case of the ⟨112⟩ diffraction spots.) The crosses indicate the diffraction peak locations expected for the unreconstructed surface. The central diffraction peaks D and K are shifted outward by $\Delta G = 0.054$ Å from the expected location $G = 2.515$ Å.

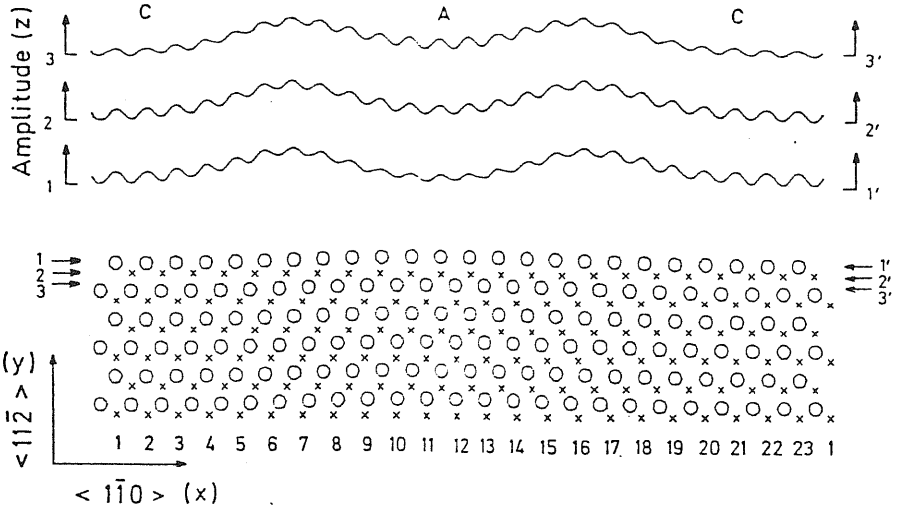

FIG. 10 Top: hard-wall corrugation functions at three points in the unit cell. Vertical scale exaggerated for clarity. Bottom: proposed structure. Crosses represent the second-layer and circles the surface-layer atoms.

periodicities. In the top layer, due to a change in electronic structure relative to the bulk, it is favoured a contraction to a smaller lattice constant, but the competing interaction with the bulk compells the surface atoms to stay in their normal bulk positions. This situation may well be a physical realization of the Frenkel-Kontorova model of competing interactions (20), already discussed in appendix 1.

The ground state of this model has been calculated by Frank and Van der Merwe (21) and one of the solutions is a lattice of regularly spaced soliton type walls ,which separe commensurate regions. The soliton superlattice can be regarded as a compromise between a fully incommensurate, and in this case compressed, structure in which the surface layer forces dominate, and an unreconstructed surface with bulk forces dominating.

The diffraction pattern doesn' t depend on crystal temperature between 120 K and 700 K. So U. Harten et al.(18) conclude that the interaction between the solitons is probably so strong that it overrides the entropy contribution to the free energy which might otherwise cause temperature-driven transitions between phases of different soliton density or disordering of the walls.

1.3 - A microscopic model for Au surfaces reconstruction: the model by Heine and Marks.

We must observe that there exists as yet no detailed theoretical description of gold surface reconstructions. Some plausible arguments have been advanced, but most of them are only speculative, without any possibility of a quantitative comparison with experiments.

As we shall show later, only some phenomenological approaches have had success; in fact to make a theory at the "ab initio" microscopic level is a very difficult task. Only Heine and Marks (17) have described a possible microscopic mechanism at the origin of contraction and expansion observed in Au (111) surfaces by Marks, Heine and Smith (16, 29). The first two observe that in the bulk noble metals Cu, Ag, Au, it is well extablished that there is a tension or opposition between two types of force (17). The first is a pairwise repulsion between the atoms due to the full d shells, the second is a multi-atom electron gas attraction due to the sp electrons and sp-d hybridization. They believe that it is the competition between these two kinds of forces that causes the complex behaviour of noble metals surfaces, expecially gold.

The detailed understanding of the electrons in the bulk allows them to infer the sense of the electron redistribution at a surface.

In the bulk, noble metals have full d shells and although they

do contribute to the cohesive energy, most of the binding comes from the partially filled sp electrons. Now it turns out from experimental studies, that the sp electrons would like to have a substantially smaller atomic volume, that is they produce a strong attraction which is balanced by the d shells that are under compression.

The theoretical reason for this is that the pseudopotential of the noble metals, particularly for the s electrons, is unusually attractive compared to alkali atoms with the same core radius R_c. The pseudopotential is normally repulsive inside the core of an atom, but in the noble metals, because of the difference in radius between the 5s and 5d orbitals, there remains an anomalously attractive region on the outer edge or "mantle" of the core. Electrons would like to flow into this mantle, hence the contractive effect of the sp electrons.

At the surface it happens that the d shells remain full and essentially unchanged, giving an expansive pressure. The sp electrons are very mobile and can relax normal to the surface and tangentially. They will lower their energy by flowing into the attractive mantle region described above. The forces that they give rise to depend sensitively on exactly where around the mantle shell they go to. For istance, if they go into the regions between the atoms in the top most layer, this increases the in-plane sp bonding and gives a tangential compressive stress.

In this paper by Heine and Marks (17), perhaps the key result is that we can reconcile apparently conflicting experimental reports of both expansion and contraction, like observed in Au (111), without any difficulty: in fact the final result is strongly dependent upon the local geometry on the surface and contractions, for istance, are not an intrinsic property of an element.

2) THE GLUE MODEL

2.1 - Necessity of a glue term

It has been known for a long time the theoretical inadequacy of the model, used to describe the cohesion of solids, according to which the metal is composed by single entities (undeformed atoms or molecules) with a pairwise interaction.

The main physical feature of a metal is the multitude of conduction electrons that constitues a sort of quantum mechanical "glue", which in no way can be taken in consideration by a pairwise model.

In spite of the absence of any theoretical foundation, the pairwise model, which arranges a center of force in every lattice position, has been for long time the only way to do many predictions at least for the bulk properties. However it has at least two big shortcomings. The first is related to the elastic behaviour of the crystal. In fact, if such a model is used, certain relations between the elastic constants can be analytically derived. These are known as Cauchy relations and for a cubic crystal, they reduce to $c_{12} = c_{44}$. But it is experimentally proved that these relations are not true in real metals.

The second shortcoming is related to the energetics of the defects formation. In a two body scheme the energy of the vacancy forma- equals the cohesive energy,but experimentally it is one third of the

of the cohesive energy.

Other examples show the total inadequacy of a pairwise interaction to describe any observed properties of metal surface, such as recon - struction or contraction of the distance between the outermost atomic planes seen by LEED (30-31). Usually the contraction is maximum for the surface layer and rapidly disappears going into the interior ones. Instead, with a two body potential, the distance between the external planes certainly increases or keeps the same value, if we restrict the interaction to nearest neighbours (32).

We conclude therefore that, in order to give a realistic de- scription of the defects formation, in particular of the observed structure of real metal surfaces, we cannot disregards the presence of the conduction electrons, whose "gluening" role can in no way be si- mulated by using a pairwise interaction. So, in order to consider the electronic effects, a many body term must be added to the interatomic two body potential. And this must be density dependent. This fact can be explained intuitively, considering that the common feature of every defect formation process, including surface, is a local change of the atomic arrangement in the zone where the defect has been created. For this reason it is important to know the various possible configurations of the "host" environment around the defect position.

Therefore it is possible to define a local host density, such that its value, in a given point, is just a measure of the presence

in that point of the other single entities, up to now and later on called atoms, which are assembled in this model to form the metal. This picture becomes much clearer if we consider, for example, that in the surface reconstruction the atoms on the outermost planes rearrange themselves under the action of some driving force. In this scheme such a force is locally created by the energy variation associated to any deviation of the host density, in a given point, from its equilibrium bulk value. As a result the atoms will move in order to restore a new equilibrium situation, which,of course, will differ from the bulk one, if some atoms have been wrenched from the metal. So in this model the equilibrium situations are always based on the balance between the many body forces and the two body ones, which are not vanishing if the atoms do not find themselves in the equilibrium bulk positions.

Once extablished the necessity of a many body term, besides a two body term, to describe the properties of a metal, we must say that several calculational schemes based on this concept have been recently described (33-37).

For istance, Daw and Baskes (33-35) notice that the pair potential method yields the total energy directly, but requires the use of an accompanying volume dependent energy (38) to describe the elastic properties of a metal. Any ambiguity about the volume may automatically invalidate the results. Such ambiguities arise in calculations

involving surfaces, for example, because the exact termination of the volume on an atomic scale at the surface is ambiguous. Relaxations, reconstructions, or defects in the surface make this ambiguity more pronunced.

Daw and Baskes (33-35) describe a new method , which they call "the embedded atom" method of treating metallic systems where fractures, surfaces, impurities can be included. This new method is based on an earlier theory "the quasi atom theory"(39). In this scheme an impurity is assumed to experience a locally uniform or only slightly non uniform environment (uniform density approximation).

In its simplest form, the energy of a quasi atom is given by

$$E_{quas} = E_z (\rho_h(R)) \qquad (2)$$

where $\rho_h(R)$ is the electron density of the host without impurity at R, the site where the impurity is to be placed, and E_z is the quasi atom energy of an impurity with atomic number z.

In the quasi atom scheme each atom in a solid can be viewed as an impurity embedded in a host, comprising all the other atoms. They can demonstrate that, because the energy of an impurity is a functional of the electron density (according to Hohemberg and Kohn (40)) of the unperturbed host, the cohesive energy of a solid can be calculated from the embedding energy. Therefore Daw and Baskes (34) take the following ansatz, based on the quasi atom concept, for the total energy

$$E_{tot} = \sum_i F_i (\rho_{h,i}) \qquad (3)$$

where F is the embedding energy, $\rho_{h,i}$ is the density of the host at the position R_i, but without atom i, and the total energy is the sum of the individual contributions. Here each atom experiences a locally uniform electron gas, and the embedding energy is defined to be the energy of that atom in an uniform electron gas relative to the atom sepated from the electron gas.

Considering also the core-core repulsion, the total energy results

$$E_{tot} = \sum_i F_i (\rho_{h,i}) - 1/2 \sum_{ij} \phi (R_{ij}) \qquad (4)$$

where ϕ_{ij} is the short range pair potential and R_{ij} is the distance between atoms i and j. Making a further semplification by assuming that the host density $\rho_{h,i}$ is closely approximated by a sum of the densities of the constituentes ρ^a ,that is $\rho_{h,i} = \sum_{j \neq i} \rho^a_j (R_{ij})$, the energy is then a simple function of the positions of the atoms. Here ρ^a_j is the contribution to the density from atom j, where $\rho_{h,j}$ is the total host electron density at atom j.

It may be interesting to see how in this scheme it is possible to compute the surface energy. This is computed by using for the contribution of each atom i to the total energy

$$E_i = F_i(\rho_{h,i}) + 1/2 \sum_{j \neq i} \phi (R_{ij}) \qquad (5)$$

For atoms in the bulk, $-E_s$ is the sublimation energy, but surface atoms will have higher energy. The difference $(E_i - (-E_s))$, summed

over all atoms and divided by the area, give the total surface energy.

Similar approaches have been also developed by M.V. Finnis and J.E. Sinclair (36) and by F. Ercolessi (41).

2.2 - The glue model by F. Ercolessi, M. Parrinello, E. Tosatti

Recently it has been developed a phenomenological (classical) many body force scheme, nicknamed the "glue" model which has proved to work very well for Au surface properties. In particular, the gross features of the Au (100) and Au (110) reconstruction (42-43) can be understood in this scheme.

It will be shown here that also some characteristics of Au (111) reconstruction can be explained within such a model.

The potential energy of the system has the form:

$$V = 1/2 \sum_{\substack{ij \\ i \neq j}} \phi (|\vec{r}_i - \vec{r}_j|) + \sum_i U(n_i) \qquad (6)$$

where

$$n_i = \sum_{j \neq i} \rho (|\vec{r}_i - \vec{r}_j|) \qquad (7)$$

is an effective coordination number which we normalize to 12 for atoms in a T=0 fcc bulk.

Let's try to understand better the meaning of the term $\sum_i U(n_i)$ in this particular glue model. This is a sum of atomic energies which are functions to be determined of the local host density n_i at the lattice positions R_i, but without atom i. We do not loose any generality considering explicitely the various contributions to the local densi-

ty

$$n_i = \sum_{j \neq i} \rho_{i,j} \tag{8}$$

Let us now do a further approximation considering n_i, the contribution to the host density at i coming from the site in j, only function of the distance $|\vec{r}_i - \vec{r}_j|$, that is

$$\rho_{ij} = \rho(|\vec{r}_i - \vec{r}_j|) \tag{9}$$

So, according to this last formula, a given atom in a certain sense sees the environment in which it takes place or it is able to count the other atoms which contribute to the host density.

It seems very reasonable to expect that , defining appropriately the many body terms U and n_i, the atoms can choose the host structure in such a way to have the lowest energy.

We can now define in detail the host density. First we observe that to justify the presence of the classical interaction ϕ , the atoms must be compact units; we choose for them a spherical shape. Further we must define for each of them a particular distance such that an atom can see all other atoms which are far from it less than such a distance, weighing them suitably. In other words, we suppose that a given atom i interacts with the other atoms j, which are in a sphere of radius R and this interaction is dependent only by their separation $|\vec{r}_i - \vec{r}_j|$ (44).

The pair potential $\phi(r)$, the atomic density function $\rho(r)$

and the glue function U(n) are all empirically constructed. $\phi(r)$, $\rho(r)$ and U(n) (fig.11) have been chosen and adjusted so that they would reproduce well a large variety of crystal properties, such as the crystal structure and lattice parameter, the surface energy, the bulk modulus, the phonon dispersion relations and the thermal expansion coefficient. Also several other properties, such as vacancy formation energy, melting temperature and latent heat turned out to be well reproduced by this choice.

We must notice that the rise of U(n) for decreasing coordinations, such as one finds at a surface provides a natural driving force for reconstruction: since the coordination of a surface is poor,it pays to reconstruct into a denser layer with better coordination.

2.3 - Molecular dynamics for the glue model

The study of the Au (100) and Au(110) surface reconstructions has been done within the model already outlined with the glue term added to the pair potential, and the optimal atomic configuration of slabs has been obtained by a molecular dynamics strategy (37,42-43).

Also for the study of Au(111) surface we adopt the same model with the same molecular dynamics technique proposed by Rahman (45-46). Now we shortly summarize it.

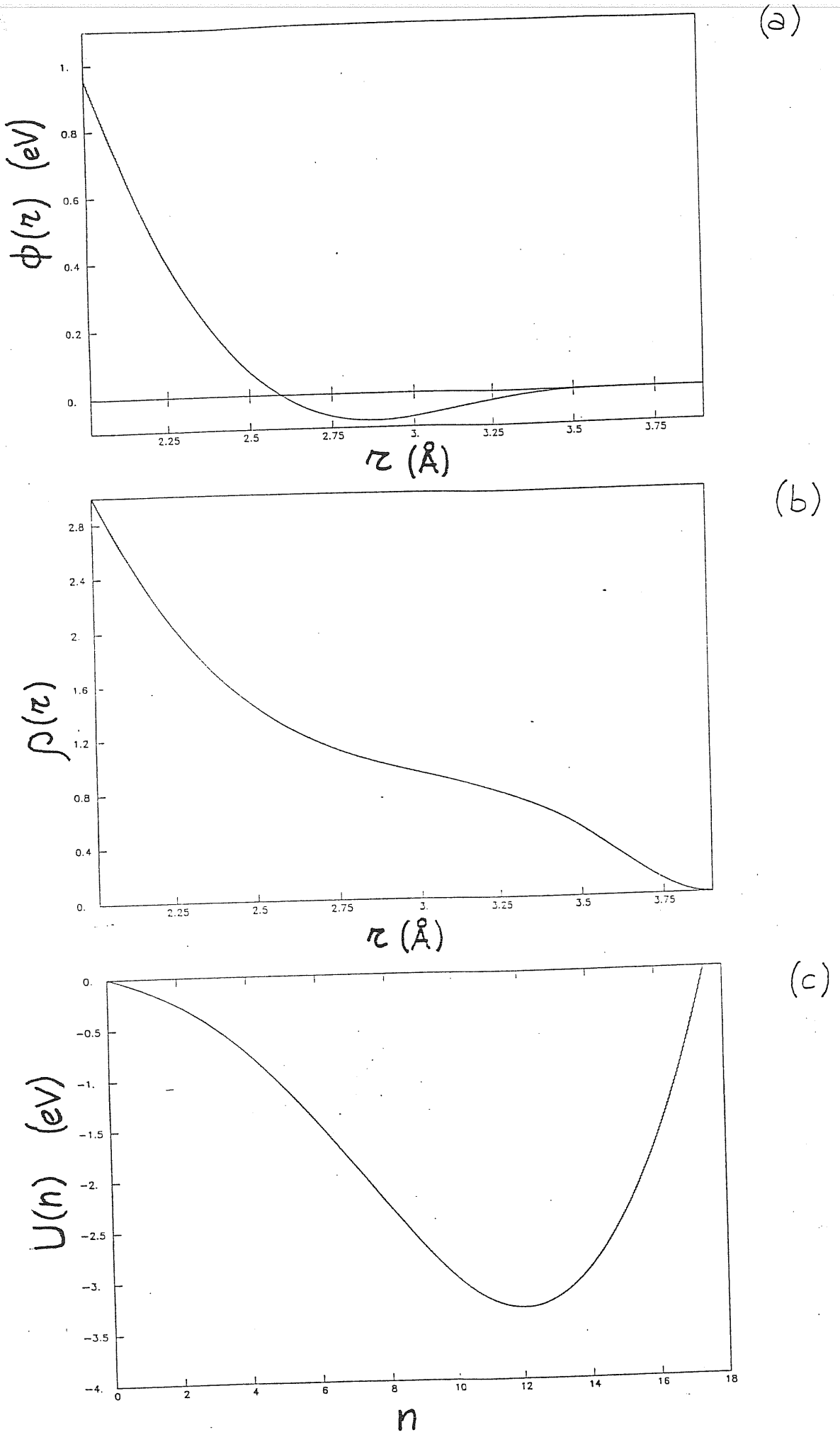
(a)
φ(r) (eV)
1.
0.8
0.6
0.4
0.2
0.
2.25
2.5
2.75
3.
3.25
3.5
3.75
r (Å)
(b)
ρ(r)
2.8
2.4
2.
1.6
1.2
0.8
0.4
0.
2.25
2.5
2.75
3.
3.25
3.5
3.75
r (Å)
(c)
U(n) (eV)
0.
-0.5
-1.
-1.5
-2.
-2.5
-3.
-3.5
-4.
0
2
4
6
8
10
12
14
16
18
n

FIG. 11

By molecular dynamics, one can manipulate the system of N interacting particles to bring it to the desired thermodynamic state.

Following Rahman (46) we observe that the only quantity which can be described is the total energy E (microcanonical ensemble). Since $E = V + \sum_i 1/2\ m_i \dot{r}_i^2$, the reduction of all $\dot{r}_i$ by a factor $\alpha < 1$ will reduce the energy E and vice versa for $\alpha > 1$. The choice of α and the frequency with which it is applied varies according to circumstances. At this point we can introduce the temperature scale for measuring the kinetic energy. Writing $\sum_i 1/2\ m_i \dot{r}_i^2 = 3NK_B T(t)/2$ we shall say that the system has a certain temperature T at time t to imply that it has total kinetic energy at time t equal to $3NK_B T(t)/2$.

The average of T(t) over a sufficiently long dynamical run will be referred to as the temperature of the system for that run.

Using this terminology, the reduction or increase in E, the total energy, is achieved by "cooling" or "heating" the system. From our understanding of statistical mechanics, we expect that the equation of state of such a system, T(E), is the dependence on E of the average temperature T of the system over a long enough time t; it is more usual to think of this relation as E(T). It is also obvious that if T(t) at any moment t is high enough the system will dissipate by a process of evaporation or explosion, depending on the circumstances.

Also the cooling of the system has some limits. Firstly, the factor α put equal to zero is the ultimate in reducing the temperature at time t to 0; however, immediately afterwards the temperature will start rising by the conversion into kinetic energy of some of the potential energy of the system at time t; thus, drastic temperature reduction cannot be achieved in one step; secondly, as the system is cooled, it gets more and more sluggish and takes longer and longer to sample the configuration space available to it.

The problem of molecular dynamics is to convert differential equations into a set of difference equations which enables us to go from time t to $t+\Delta t$ with a suitably chosen Δt. This can be done with various algorithms.

In this calculation it has been used a predictor-corrector algorithm, which can be found in a report by Gear (47) and which we describe in appendix 2.

For what concerns the calculations of the forces, we must say that this being the most time consuming part of the whole calculation, particular attention has to be paid so as to make it as efficient as possible. If for istance, speaking in general, the potential is given to be a sum of two-body potentials, depending on the pair distance alone

$$V = \sum_i \sum_{j>i} \phi_{ij}(r_{ij}) \qquad (10)$$

the force on i due to j is

$$-\nabla_i \Phi_{ij}(r_{ij}) = -\left(r_{ij}^{-1} \frac{d\Phi_{ij}}{dr_{ij}}\right) \vec{r}_{ij} \qquad (11)$$

If r_{ij} depends on even powers of r only, then $-1/r_{ij}\,\Phi'_{ij}$ also has only even powers which makes for a great saving, since no square root calculations need to be performed. However, for any function Φ_{ij} one can use this advantage (of not having to calculate square roots) by tabulating the function not as a function of r, but of r^2. The calculation of the forces thus proceeds by programming the double sum as indicated above with $j > i$ (rather than $j \neq i$ and 1/2 to go with it, calculating r_{ij}, its square r_{ij}^2, the value of Φ'_{ij} and $r_{ij}^{-1}\,\Phi'_{ij}$ and finally the three numbers $(r_{ij}^{-1}\Phi'_{ij})\vec{r}_{ij}$ which gives the components of the force on i due to j. The same values with changed signs give the force on j due to i. Thus we get for the forces:

$$\vec{f}_i = -\sum_{j\neq i}^{N}{}_j \nabla_i \Phi_{ij}(r_{ij}) \quad i = 1,2,\ldots N \qquad (12)$$

It has been used the following procedure invented by Verlet, that is useful when dealing with moderately large systems like the system which we have considered. For very small systems (N from 100 to 200) such procedures are not of any use, and for very large systems (N from 5000 to 10000) further elaboration of the procedure becomes necessary.

Unless one is dealing with very dilute systems (for which molecular dynamics becomes a doubtful method of investigation) one can state that for several Δt of molecular dynamics, the neighbours up to distance r_c, which is linked to the cutoff of the potential will be, in large majority, unchanged. A few move out of range r_c and a few will move within range. Thus, if at any moment we construct a list of neighbours not up to r_c, but up to r_c+S, where S denote a skin tickness, then for several Δt after that moment, we need to consult only this list (and not the whole system) to identify the neighbours up to r_c and to throw away those beyond r_c. It would be shown also that there is an optimum balance between the value of S and the number of Δt for which the list, once made, may be used.

For molecular dynamics, it remains to consider the usual periodic boundary conditions (pbc) that enable us to extend a parallelopiped box to infinity by an integral number of translations in the three directions. This is a general consideration, but in the particular case of a slab, we have imposed pbc only in the x and y directions, not in the z direction. This implies, for istance, quantized values of k_x and k_y in the x and y direction, not in the z one.

Intuitively one can observe that for potential functions which are short ranged, compared to half the box size, the effect of pbc will be rather small.

In visualizing a system with pbc, it may be convenient to think in terms of a "box" with walls and particles "entering" from one face when "living from the opposite face. However,since the box can be drawn anywhere in space, as long as it has the correct size and it is never tilted, one can always think of any particle as being at the center of the "box" rather than at one face or another. Both ways of visualizing pbc are equally valid.

Another consideration to do is that, when a particle goes beyond $\pm$ L/2, where L is the measure of the box supposed cubic, it has to be reset so as to bring it back into the box from the opposite face. This operation simply recognizes that the image is already in the box and transfers the particle tag to its image.

3) AU (111) RECONSTRUCTION IN THE GLUE MODEL

3.1 - Au (111) reconstruction at T=0

Now we want to investigate all details concerning both shape and energetics of the Au (111) atomic arrangement, as predicted by the glue Hamiltonian at T=0. To this end we have proceeded to study the surface energy of a series of 10 layers slab with periodic boundary conditions along x and y.

The surface energy is defined as $\sigma = \frac{E - N\varepsilon_c}{2A}$ where E is the total energy of the slab, ε_c the cohesive energy per atom, N the number of atoms, A the area of the slab and the factor 2 accounts for two surfaces. We have verified that the two surfaces behave almost identically,structurally and energetically.

The size of the periodically repeated cell was $MxN\sqrt{3}$ (in units of a/ 2 where a = 4.07 Å is the T=0 lattice parameter). M is the size in the (110) direction, $N\sqrt{3}$ in the (112) one.

As in the case of (100) Au surface (37,42), we have searched the lowest energy state by a simulated annealing strategy based on molecular dynamics. Each annealing run started from few Kelvin degrees with a reconstructed $MxN\sqrt{3}$ 10 layers slab. The topmost layer was a perfect triangular lattice contracted only in the x direction to accomodate M+1 rows onto M and not in the y direction, where there is no reconstuction according to experimental results. All the initial interlayers distance was set equal to $a/\sqrt{3}$ = 2.35 Å.

The annealing procedure consists of gradually extracting kinetic energy from the system until a local energy minimum is attained. But we must admit that this procedure offers no guarantee that the resulting local minimum is indeed the absolute minimum. In fact, changing the initial registry respect to a perfect fcc structure, or changing the initial value of the temperature for the annealing, we noted some little differences in obtained values for the minimum surface energy. Anyhow the differences among them are very little, especially compared with the difference in energy between the value of the reconstucted surface and the unreconstructed one.

In the case of (100) surface the even and odd M cases are distinguished.The odd M case, in fact, gives systematically a higher surface energy.

We don't to have to do such a distinction for the Au (111) case, where we see a regular decreasing of surface energy σ , if M increases.

We have got the minimum value at M=11 for various N; the surface energy in the case $11x2\sqrt{3}$ is lightly lower than the other $11xN\sqrt{3}$ cases. We can summarize our results:

Cell	Surface energy ($ev/A^{\circ 2}$)
$3x2\sqrt{3}$	0.0965629
$5x2\sqrt{3}$	0.0993860
$6x2\sqrt{3}$	0.0932323

$7x2\sqrt{3}$	0.0904223
$8x2\sqrt{3}$	0.0890887
$9x3\sqrt{3}$	0.0884695
$10x2\sqrt{3}$	0.0882841
$11x2\sqrt{3}$	0.0881802
$12x2\sqrt{3}$	0.0882538
$13x3\sqrt{3}$	0.0883895
$22x3\sqrt{3}$	0.0881802
$23x2\sqrt{3}$	0.0902078
$11x2\sqrt{3}$	0.0881802
$11x3\sqrt{3}$	0.0881927
$11x5\sqrt{3}$	0.0881968
$11x6\sqrt{3}$	0.0881930

It may be interesting to point out the fact that we get the same surface energy, if we consider a cell $(11x2\sqrt{3})$ with 12 rows on 11 in the first layer and a cell $(22x2\sqrt{3})$ with 24 rows on 22; in the second case, we have just taken a cell equal to the double of the first case; so we have the confirm that the smallest molecular dynamics cell is really $(11x2\sqrt{3})$ and, in every case, we can expect to obtain the same value for surface energy, if we consider molecular dynamics cells which are a multiple of the above mentioned elementary cell.

So in this model the superstructure is $(11x2\sqrt{3})$ and not $(px2\sqrt{3})$ with p = 22-23, like some experimental studies suggest.

As we have already said, we can get also a somewhat lower surface energy value if, for istance, we start from 100 °K for the quench (σ = 0.0881681 ev/Å^2) or 600 °K (σ = 0.0881561 ev/Å^2), or changing something in the initial configuration respect to the configuration of a perfect fcc crystal. For istance, among some different results obtained giving different displacements from the structure of a perfect fcc lattice, we have got the minimum value σ = 0.0881420 ev/Å^2 in correspondence of a shift in x direction equal to 0.009 Å and a shift in y direction equal to 0.333 Å.

In all these cases we can note little differences in the structure of the surface in the fundamental states. Anyhow, according to He-atom diffraction experiments, we can distinguish well in every case an area in which the structure is fcc (ABC stacking) and another in which is hcp (ABA stacking). These domains are separated by regions in which the atoms in the first layer are in bridge with the atoms of the second layer (that is, the atoms in the first layer are in the center of the line joining the centers of two atoms of the second layer).

This can be compared with the model proposed by U. Harten et al. (18), where the transition between fcc and hcp domains is described by a gradual x-dependent shift (x along (110) direction), given by the soliton expression mentioned in paragraph 1.2 and in appendix 1:

$$f(x) = 2/\pi \ \text{arctg} \left(\exp \frac{x}{\Delta S}\right) \qquad (13)$$

As it has been remarked, there are some very little differences in the possible obtained structures at T=0.For istance, in the surface with σ = 0.0881802 ev/$\mathring{A}^2$ and σ = 0.0881561 ev/$\mathring{A}^2$ the centers of the regions fcc and hcp and of the solitons don't pass through the centers of the atoms, but among them. Instead, in the surfaces with σ = 0.0881681 ev/$\mathring{A}^2$ and σ = 0.0881420 ev/$\mathring{A}^2$ the centers of the regions hcp and fcc and of the solitons pass through the centers of the atoms (figg. 12-15).

In the Au (100) surface reconstruction the presence of solitons was outlined (centered rectangular lattice) and their $\varphi_n = \frac{2\pi}{b}(x_n - nb)$ phase shifts were calculated (37,42).

Also for Au(111) surface we have calculated the phases φ, but in this case we have got almost a linear dependence, with only two very small regions in which the curve is almost plane. That means that the presence of solitons is less pronunced than in Au (100) case. In other words, we could expect a phase with a shape equal to that of a soliton with two extended regions in which is almost plane, but we have got a soliton distributed all over the cell.

We have studied the phases with final and average coordinates and we can say that with final coordinates the phases have less linear trend than the phases with average coordinates.

However, we can conclude that also in the Au (111) case, it is

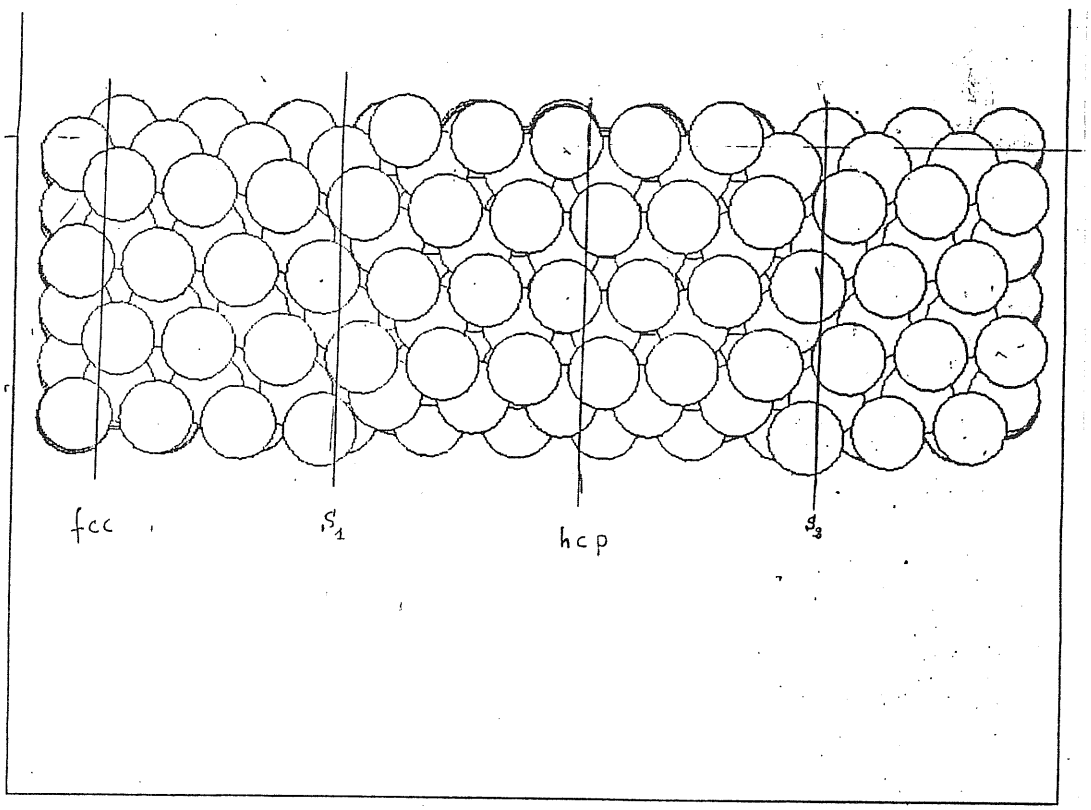

REF (111) 11x2 RECONSTRUCTED - YAP053 - QUENCHED
Top view

T = 0 0 K

$\sigma = 0.0881802$ eV/Å^2

FIG. 12

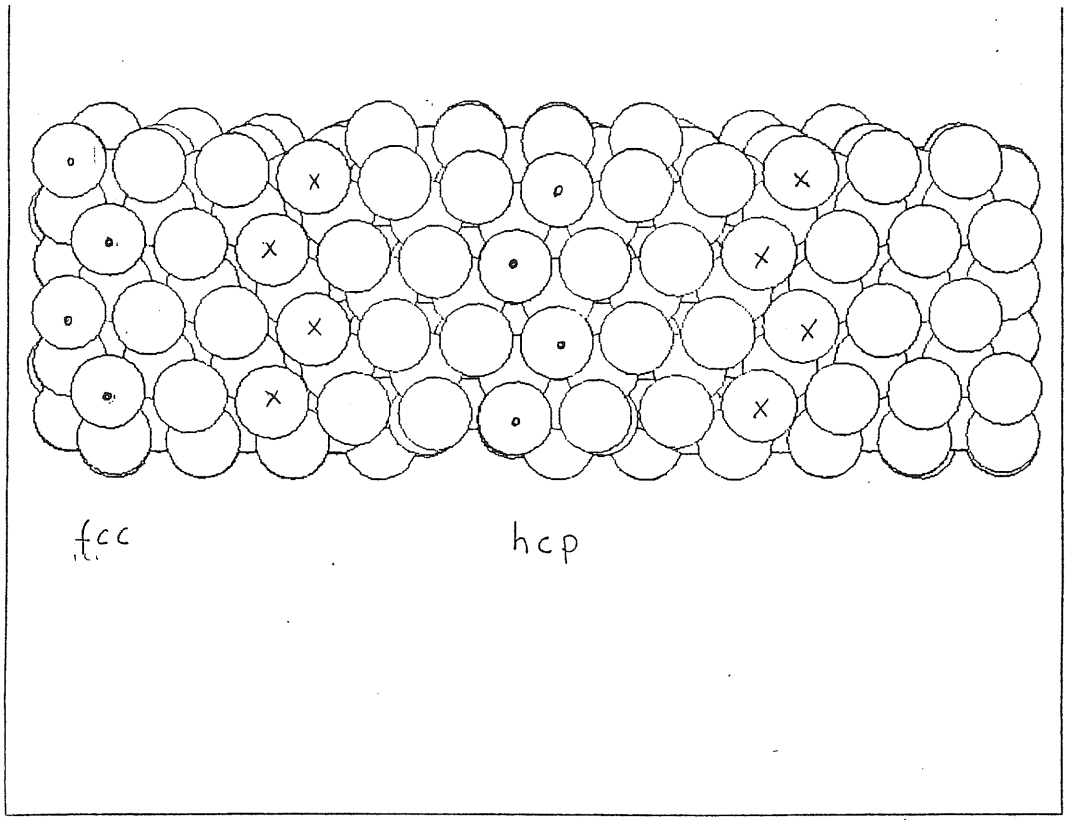

REF (111) 11x2s1 shiftx=0 00909 y=0 33333 - QUENCHED
Surface -

RADIUS = 1 199

T = 0 0 K
$\sigma = 0.0881420$ eV/Å^2
AVERAGE COORD

FIG. 13

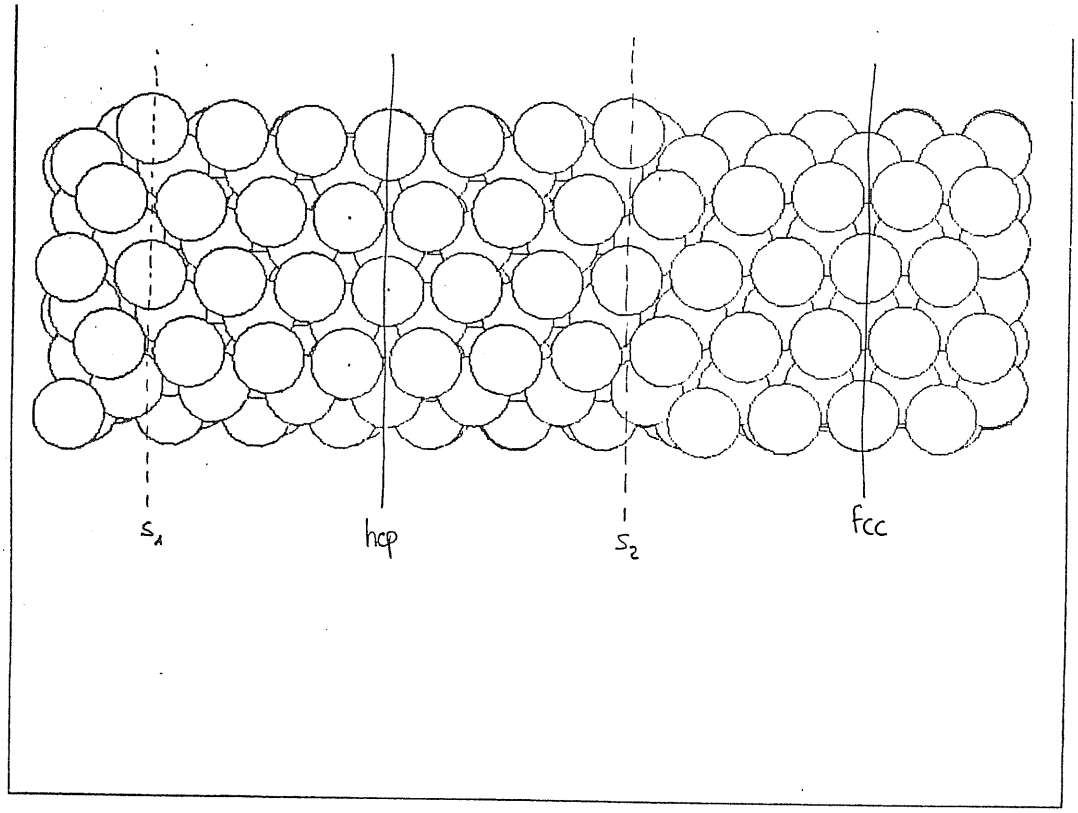

FIG. 14

(111) 11x2 QUENCH FROM 100K - QUENCHED

T = 0 0 K

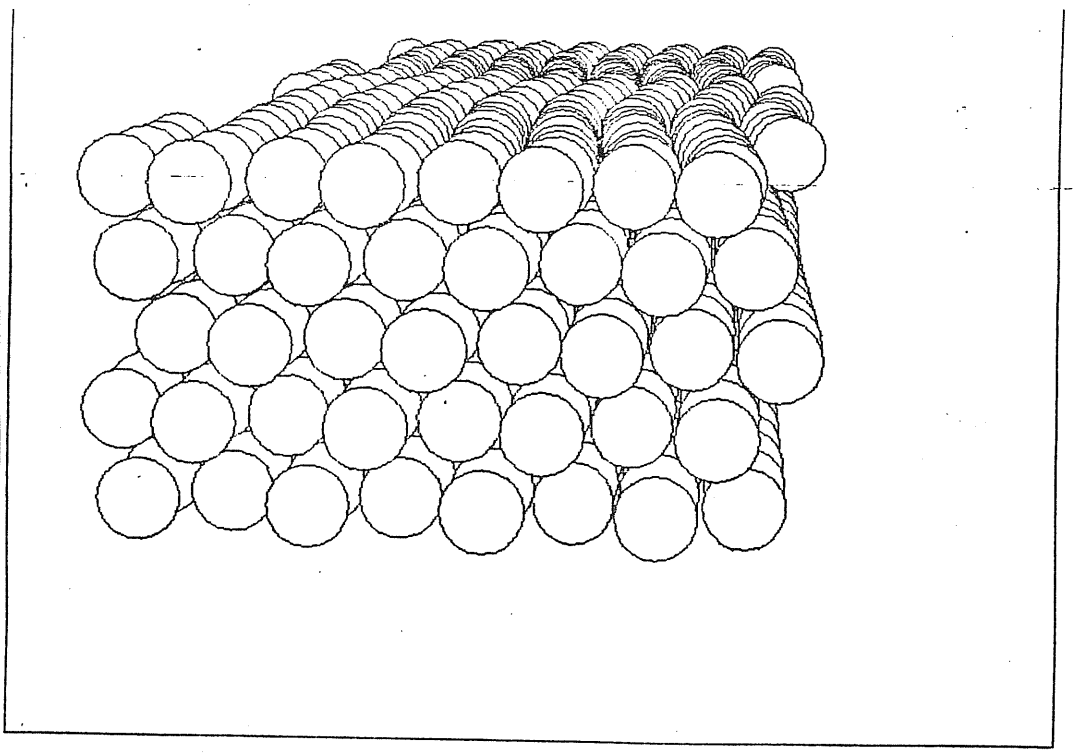

FIG.15

(111) 11x2 QUENCH FROM 100K - QUENCHED

T = 0 0 1

apparent that the strain in the x direction is concentrated in corrugated regions which have a one dimensional soliton appearance. This is evident also from the z(x) corrugation.

3.2 - Study of Au (111) surface with temperature

We have then tried to see which changes can occur in the structure of Au (111) surface rising temperature.

It should be remarked at once that we have done calculations with temperature, following the hypothesis that the lowest energy configuration is $(11x2\sqrt{3})$ also at temperatures different from zero. Really, to be correct, we should calculate free energy at every temperature and for each temperature find the correct minimum energy configuration.

As a first thing we must specify which modifications we have done in molecular dynamics scheme to take in account temperature effects. At the beginning we have changed the parameter a, that is the lattice spacing (fig. 16). Then we have done the first series of calculations with temperature different from zero with the smallest cell $(11x2\sqrt{3})$, reaching a first equilibration temperature with 500 molecular dynamics steps. The first series of steps was followed by a second series of 1500 steps to reach the fixed equilibrium temperature.

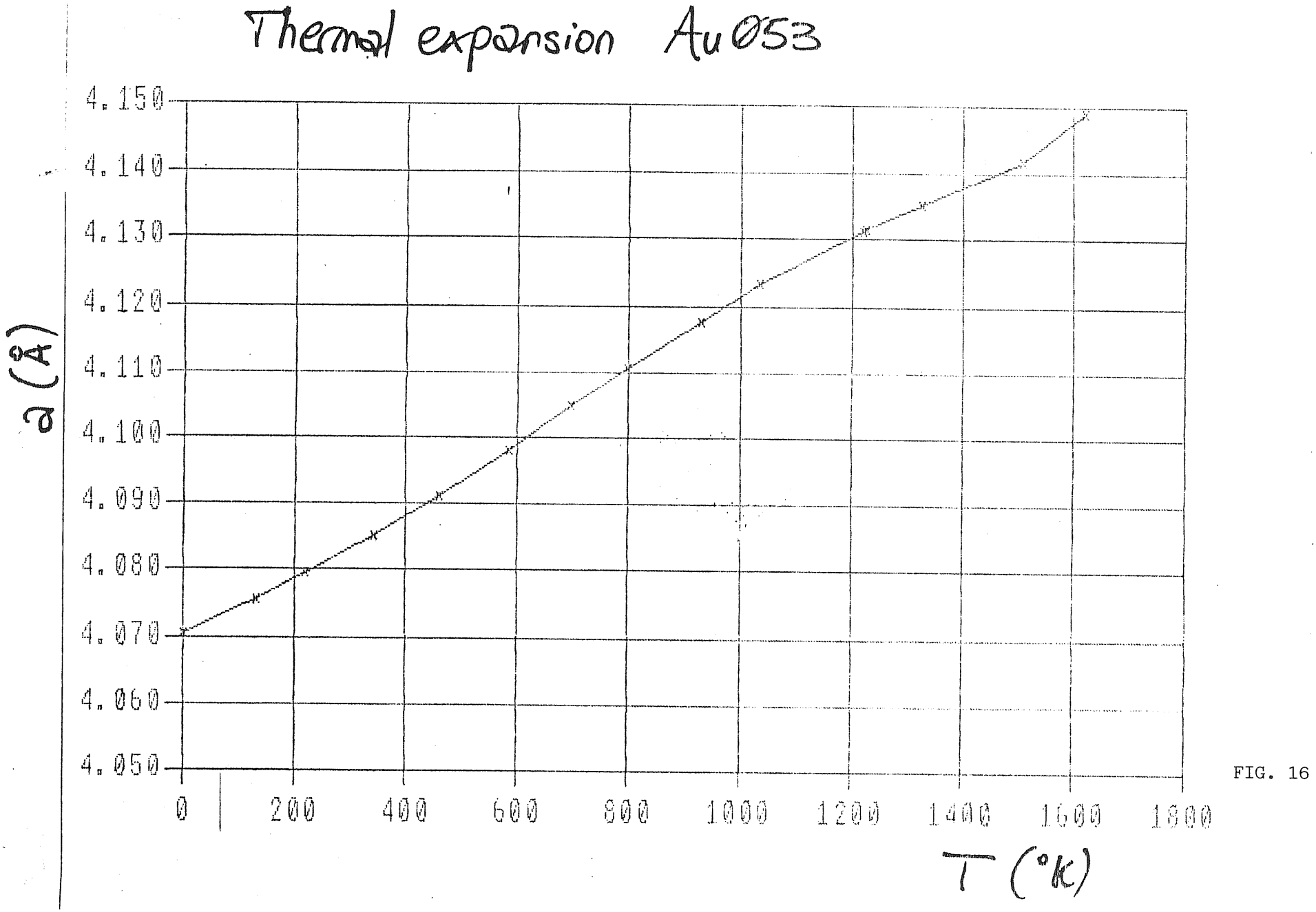
Thermal expansion Au053
4.150
4.140
4.130
4.120
4.110
4.100
4.090
4.080
4.070
4.060
4.050
a (Å)
0
200
400
600
800
1000
1200
1400
1600
1800
T (°K)

FIG. 16

So we have increased temperature by one hundred degrees every time, until 1500 °K.

We must say that we have not observed big differences, rising temperature, in the phase φ of solitons and in the structure of the surface. For what concerns the phases φ, calculated using both average and final coordinates, we can say that they do not show important variations with temperature. Especially the phases calculated with average coordinates have more and more linear shape, if the temperature increases. The same happens for phases calculated with final coordinates, even if these have a little less regular shape.

As it regards the variations of the structure studied with final coordinates (snapshots), also at high temperatures we could always distinguish the domains fcc and hcp and the regions of solitons (rows of atoms in bridge with the second layer) even if we can say very qualitatively a little disordered.

This means that such a structure, that is such a reconstruction is very stable. In fact we have already said that the reconstruction lasts until 900 °C (14), as it follows from experimental results.

So to study better the region of high temperature, where we can expect the phase transition, we have taken a much bigger molecular dynamics cell, taking in x and in y one multiple of the supercell ($11x2\sqrt{3}$) which, as already noted, gives, in this model, the minimum surface energy. We have chosen before a ($22x2\sqrt{3}$) and then a

a $(22x10\sqrt{3})$ cell.

With the $(22x2\sqrt{3})$ cell we had 896 moving particles in 10 layers. We have tried to work with some layers with fixed particles to reduce the number of moving particles, in particular we have blocked particles in 6 layers among 10, getting so only 448 moving particles with 96 particles in the first layer. We have repeated the calculation at different temperatures with blocked and not blocked particles and have not got qualitative differences between the two cases.

For the case $(22x10\sqrt{3})$, as we had some problems of size because we had too many particles moving, we have used the program with only 5 layers and 2 had fixed particles. Therefore we have reduced from 2240 to 1360 our number of moving particles and we have worked with 480 particles in the first layer. We must note that the extension in the y direction permit to observe very well the undulation in this direction.

With this big system we have found that until 1400 °K it is possible always to recognize well the presence of domains fcc, hcp and the walls of solitons, even if disordered; over 1400 °K, instead, we have observed the formation of dislocations and it is not more possible to recognize well the walls of solitons (figg. 17-22).

We must remark that this model with the chosen number of molecular dynamic steps doesn't previde the right melting temperature, but a much higher one.

Very recent calculations (48) have shown that in this glue model the bulk melting temperature is 1355±10 °K.

In our calculations the system in not yet melted at 1500 °K. In fact, to obtain the right melting temperature, it was necessary a number of steps of the order of 10000, while we have not gone besides 2000 steps for a first equilibration followed by other 3000 steps. So what we have got is, in reality, only a metastable state, not effectively a stable equilibrium state.

Anyhow this fact doesn't prevent us from studying the changing of the structure with temperature.

The structure of the surface, as already noted, is very resistent to temperature. The glue permits, by the reconstruction, that the system is overheated without the melting of the surface. In an unreconstructed surface, in fact, it should be easier to reach the melting point; it is just the stable reconstruction, energetically favoured, which prevents the atoms from moving from their equilibrium positions on the surface and, consequently, also in the bulk.

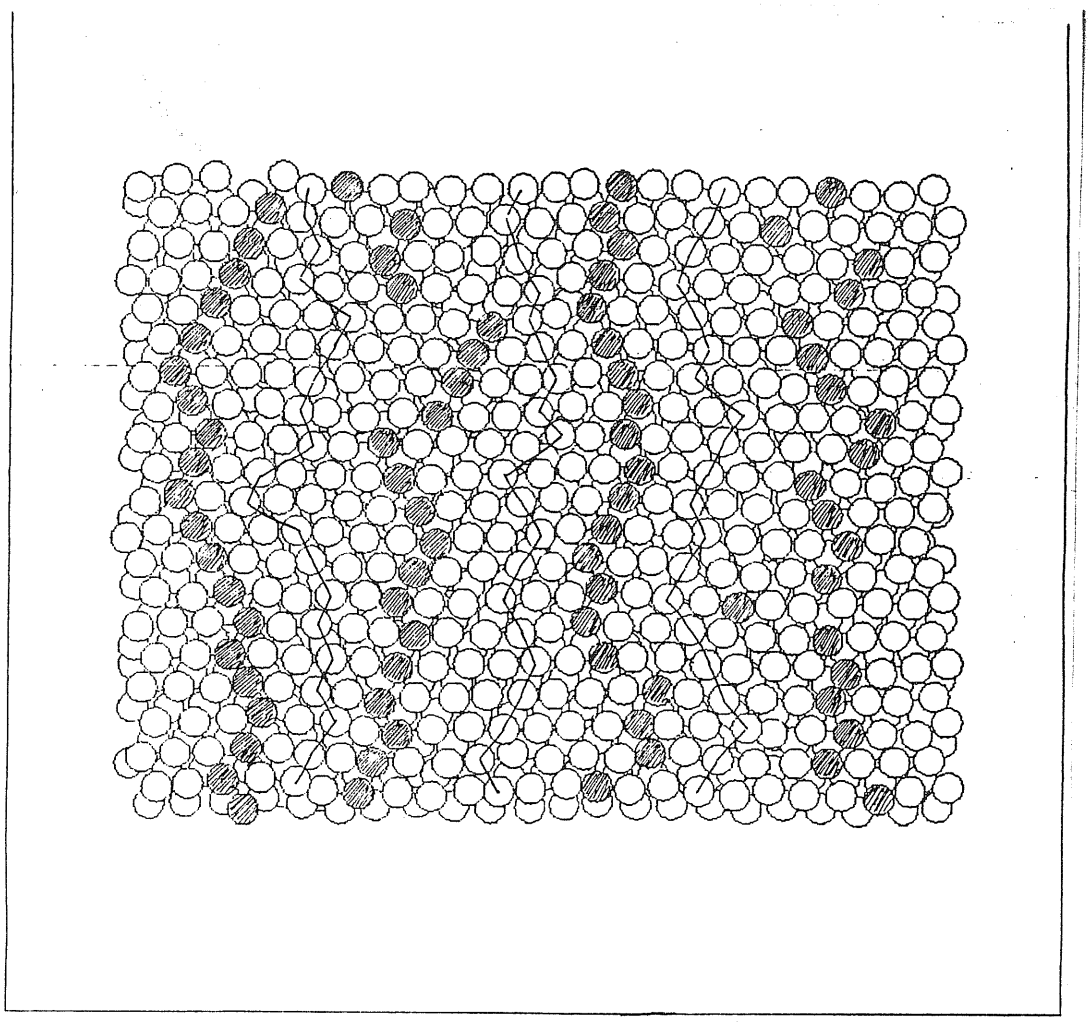

REF (111) 22X10 RECONSTRUCTED - 900K EQUILIBRATION

T = 901 9 K

FINAL COORD

FIG. 17

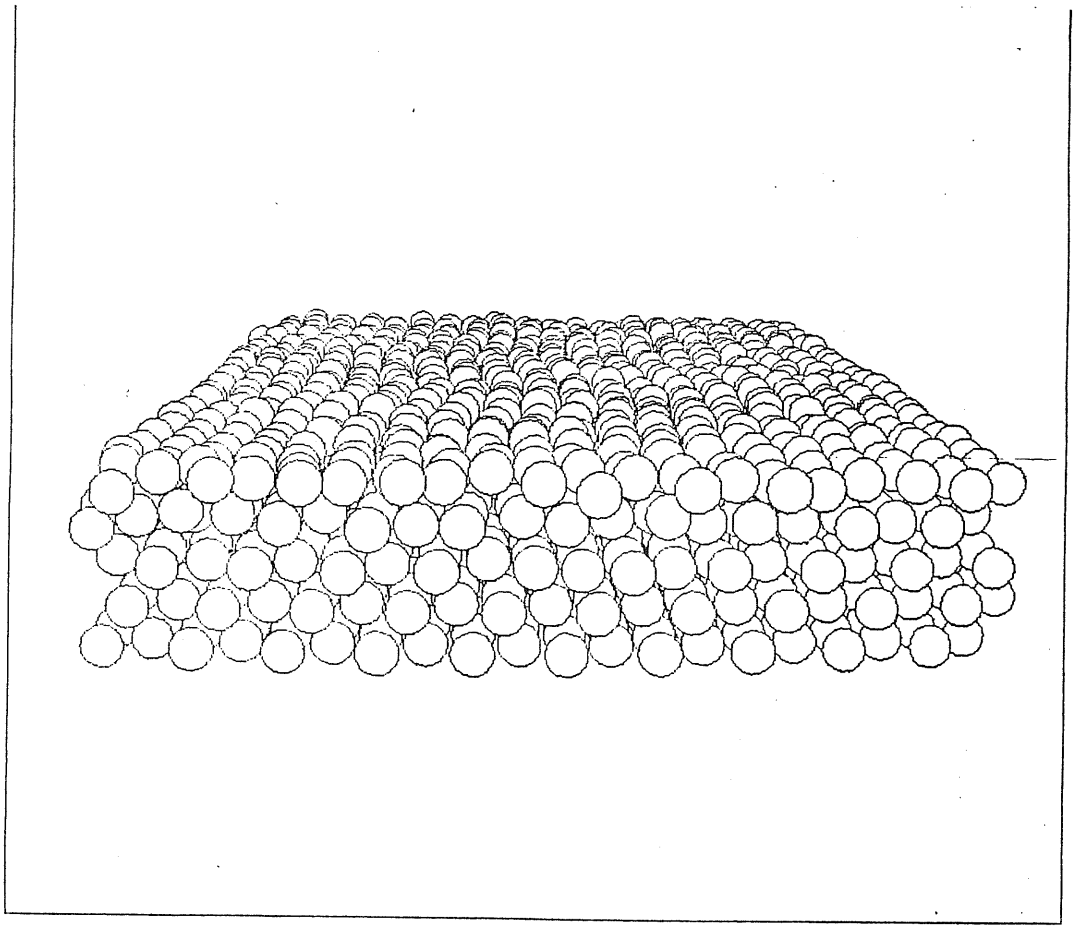

REF (111) 22X10 RECONSTRUCTED - 900K EQUILIBRATION

T = 901 9 K

FINAL COORD

FIG. 18

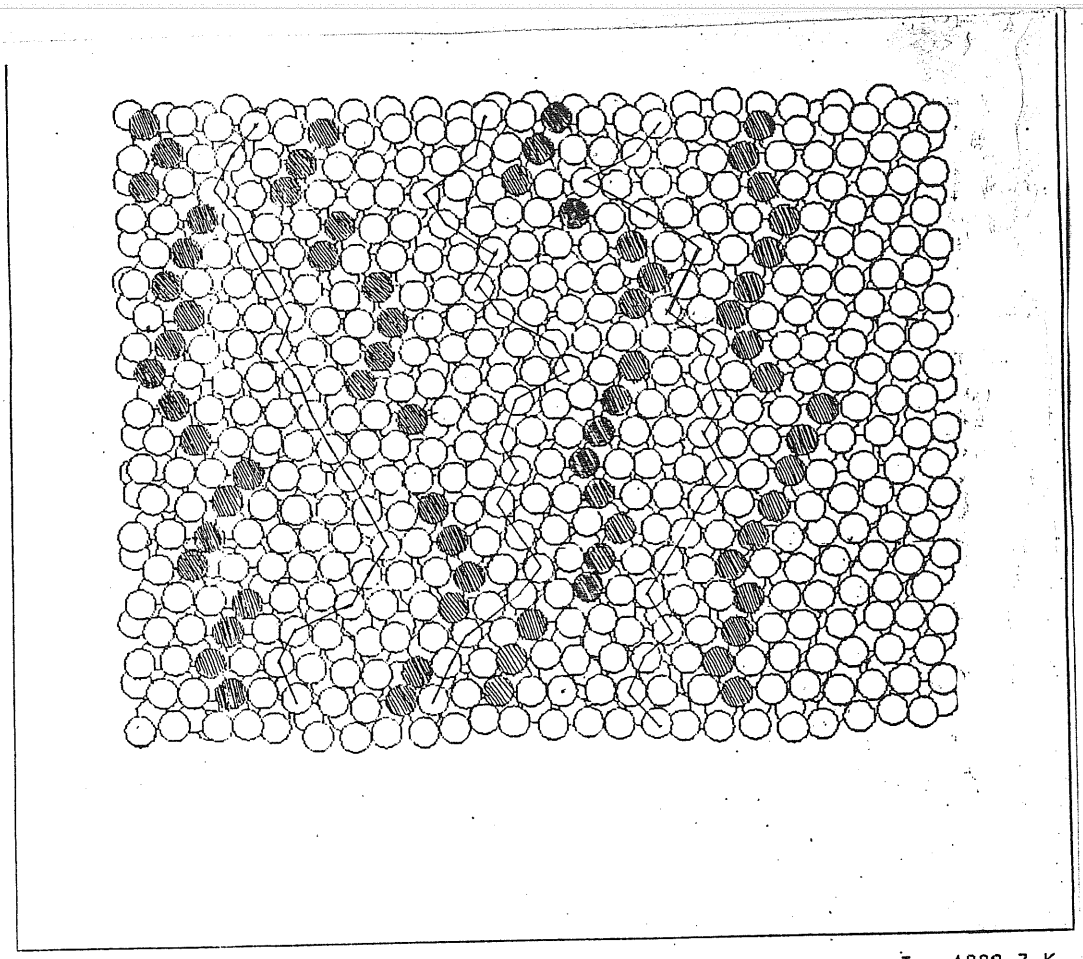

(111) 22X10 RECONSTRUCTED - 1100K EQUILIBRATION

T = 1088.7 K

FINAL COORD

FIG. 19

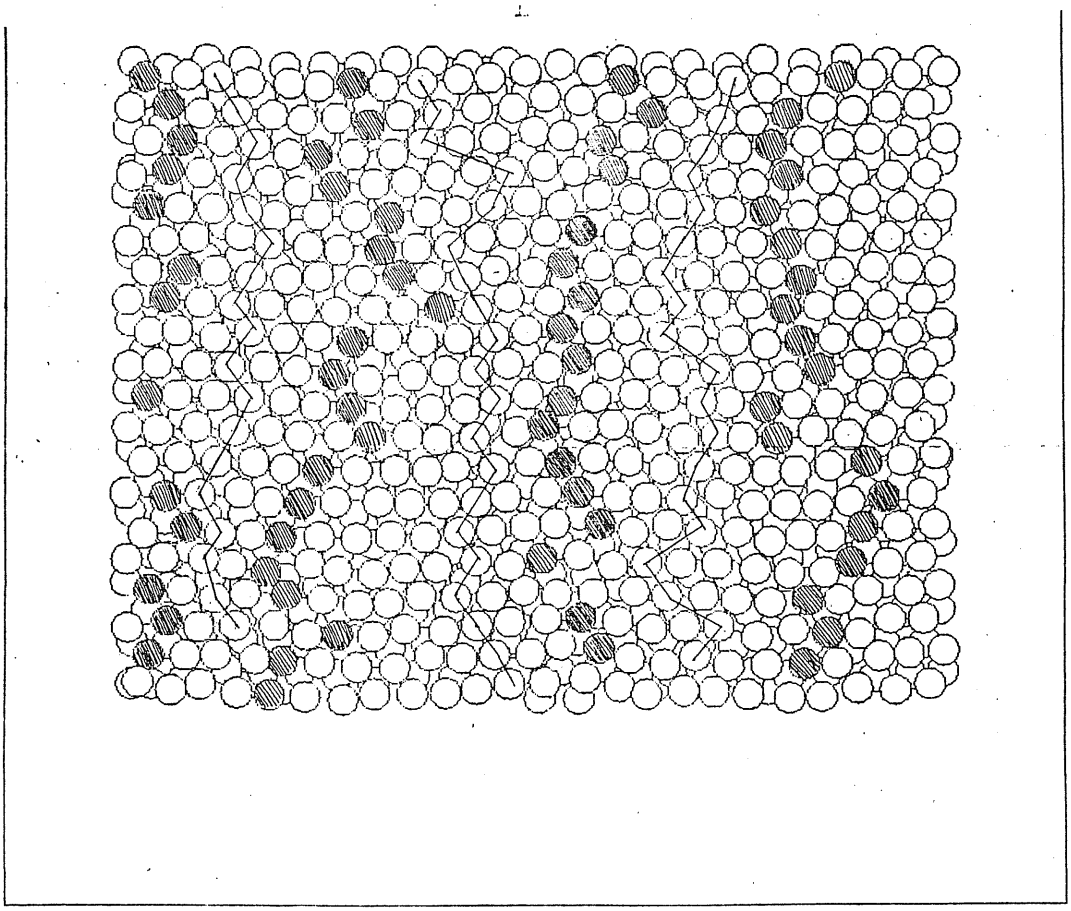

REF (111) 22X10 RECONSTRUCTED - 1300K EQUILIBRATION

T = 1297.8 K

FINAL COORD

FIG. 20

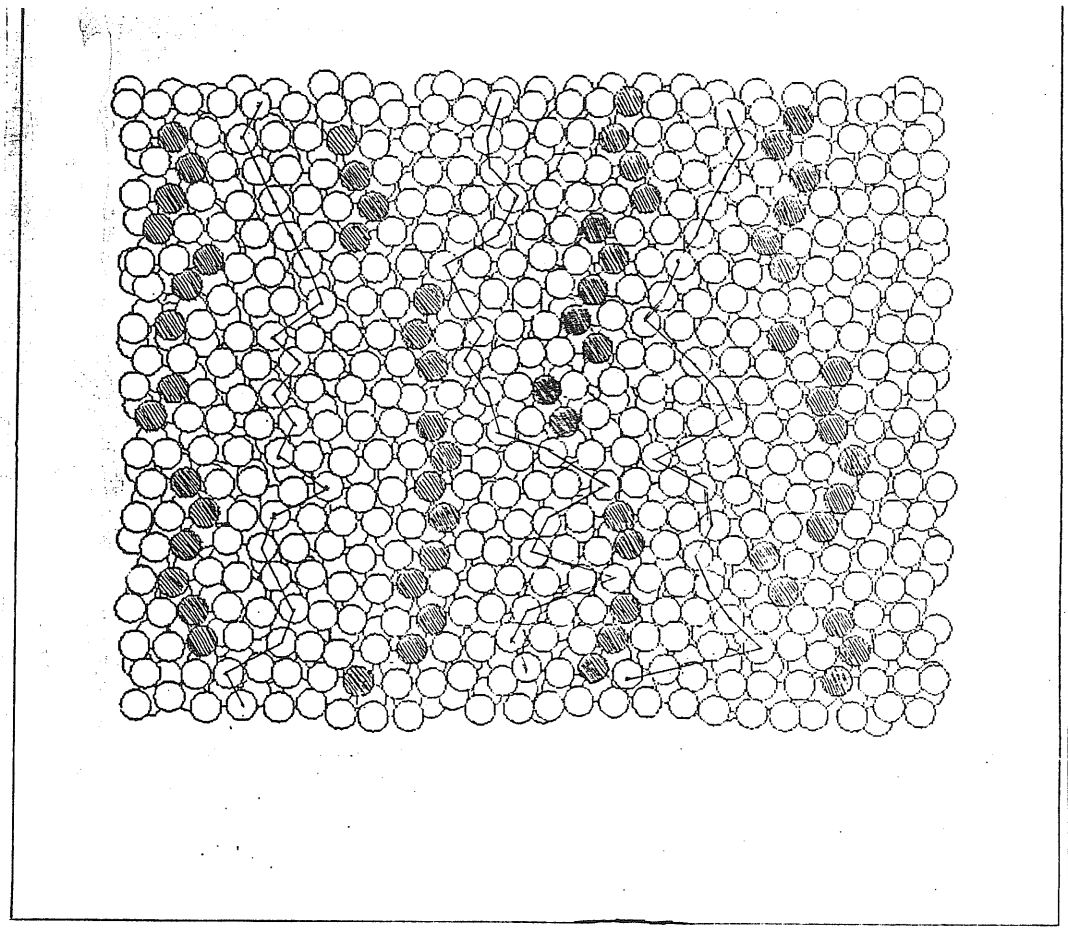

(111) 22X10 RECONSTRUCTED - 1400K EQUILIBRATION

T = 1400.8 K

FINAL COORD

FIG. 21

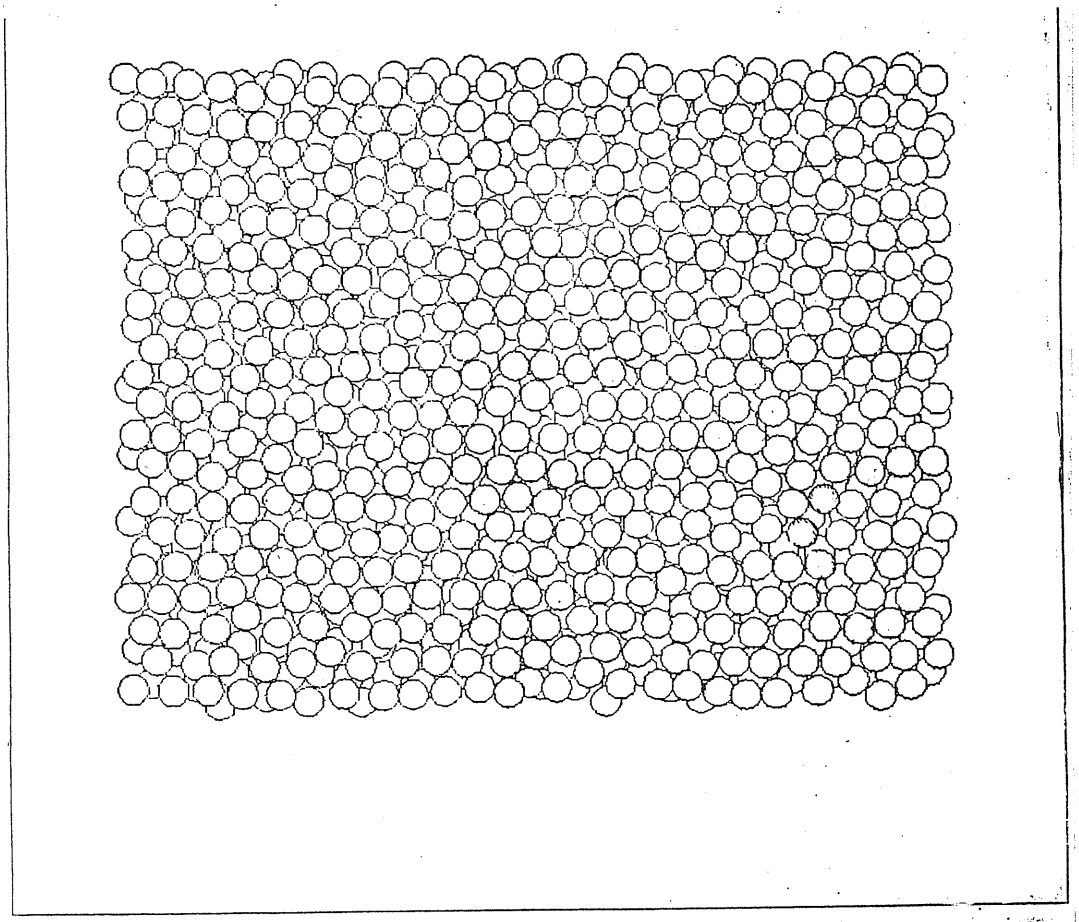

(111) 22X10 RECONSTRUCTED - 1500K EQUILIBRATION

T = 1506.5 K

FINAL COORD

FIG. 22

3.3 - Static structure factor

We have investigated the changing of structure of Au (111) surface with temperature, also calculating at the various temperatures the static structure factor

$$S(\vec{K}) = \frac{1}{N} \left\langle \sum_i e^{i\vec{k}\cdot\vec{r}_i} \sum_j e^{-i\vec{k}\cdot\vec{r}_j} \right\rangle \qquad (14)$$

With the usual boundary conditions in x and in y directions choosing a molecular dynamics box of size L_x and L_y, we have used quantized values for $K_x = \frac{2\pi}{L_x} n_x$ and $K_y = \frac{2\pi}{L_y} n_y$ and not quantized values for K_z.

We could expect that for some K values, linked to the periodicity of of the reconstruction with solitons, S(K,T) was a decreasing function for certain values of K, besides the values linked to the Bragg peaks, and an increasing function of temperature for other values of K, in such a way that all S(K,T) would converge to the same value at high temperature. But we have got generally only an increasing trend of the structure factor with temperature and we have not found particularly significant values of K to analyse.

We have studied the static structure factor choosing the K vector in the x and in the y direction, and then taking for K also one component along z, so that S(K) becomes sensible to the corrugation of the surface in the z direction.

At T=0 in the various configurations obtained, $S(K_x)$ does

not show one peak only in correspondence of the Bragg peaks, like we would have for an unreconstructed structure, but one peak circumdated by other smaller ones (fig.23). These can be linked to the reconstruction. The values of S(K) at the Bragg peaks at T=0 are equal to the number of particles in the first layer.

We observe that the Bragg peaks are decreasing in value with temperature, but for the other values of K_x, $S(K_x)$ increases. Only for low values of K_x, in the region around 900-1000 °K there is a light decreasing of $S(K_x)$, if the temperature increases. Perhaps it can be related to some little changes in the structure.

The calculation with $(11x2\sqrt{3})$ has shown that the shape of $S(K_x)$ doesn't change until the highest temperatures (figg. 24-28).

If we examine $S(K_x, K_z)$ with $K_z \simeq 5\ \text{Å}^{-1}$, like suggested from experiments (18), we can take in account the corrugation of the surface in the z direction too and we see, also at low temperatures, for very low values of K_x, high peaks. They haven't a regular trend with temperature, because the peaks in some temperature intervals decrease while in other increases (figg. 29-34).

For what concerns $S(K_y)$ and $S(K_y, K_z)$, we observe one maximum for $n_y = 4, 8, 12$ and the most pronunced is the peak for $n = 4$. This is decreasing with increasing temperature. We do not note particular changes in the shape of $S(K_y)$ and $S(K_y, K_z)$ with temperature because

in the y direction there is no reconstruction and so the structure factor is less sensible to changes in temperature. We must observe that at low temperatures there are maxima until n_y = 16,20, but at high temperatures, where the disorder increases, we have no more peaks at n_y = 12, but only for n_y =4,8.

We have repeated the calculation of the structure factor at some temperatures with bigger systems ($22x2\sqrt{3}$). We can say that qualitatively there are not big differences in the shape of the structure factor in systems with ($22x2\sqrt{3}$) or ($11x2\sqrt{3}$) molecular dynamics cell.

Therefore we have the confirm that, at least for qualitative informations, we can use ($11x2\sqrt{3}$) cell.

Anyhow, for studying the high temperature region, we have analysed also the structure factor for very big systems(($22x10\sqrt{3}$) cell).

We have prepared before a champion at 900 °K certainly well equilibrated (we have done 2000 steps for the initial equilibration and then other 10000 steps) and we have started from this for studying higher temperature region. Also in this case we have got the same information about the shape of the structure factor as in the study done with smaller molecular dynamics cells.

For what concerns $S(K_y)$ and $S(K_y,K_z)$, the maximum appears now every n_y =20, as we could expect.

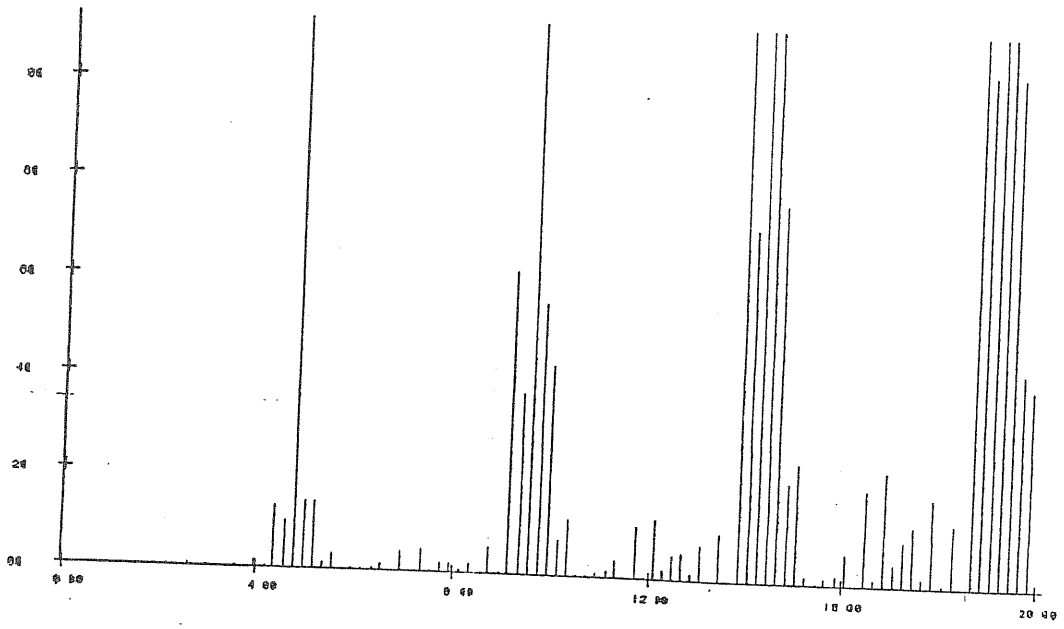

$S(K_x)$
T=0
quench from 100 K
FIG. 23

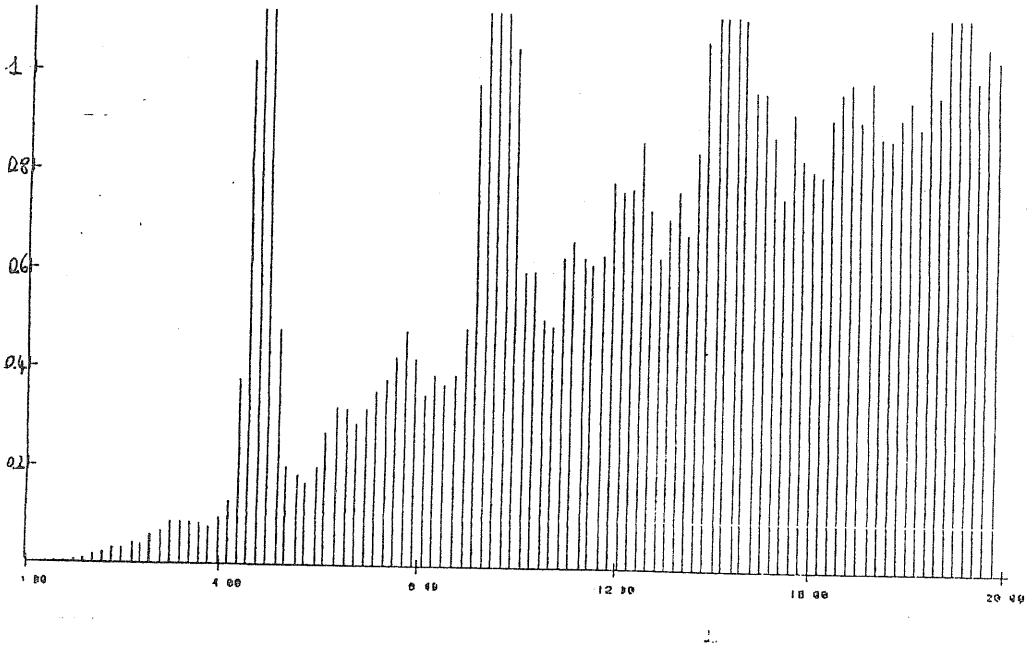

FIG. 24

T = 300 K

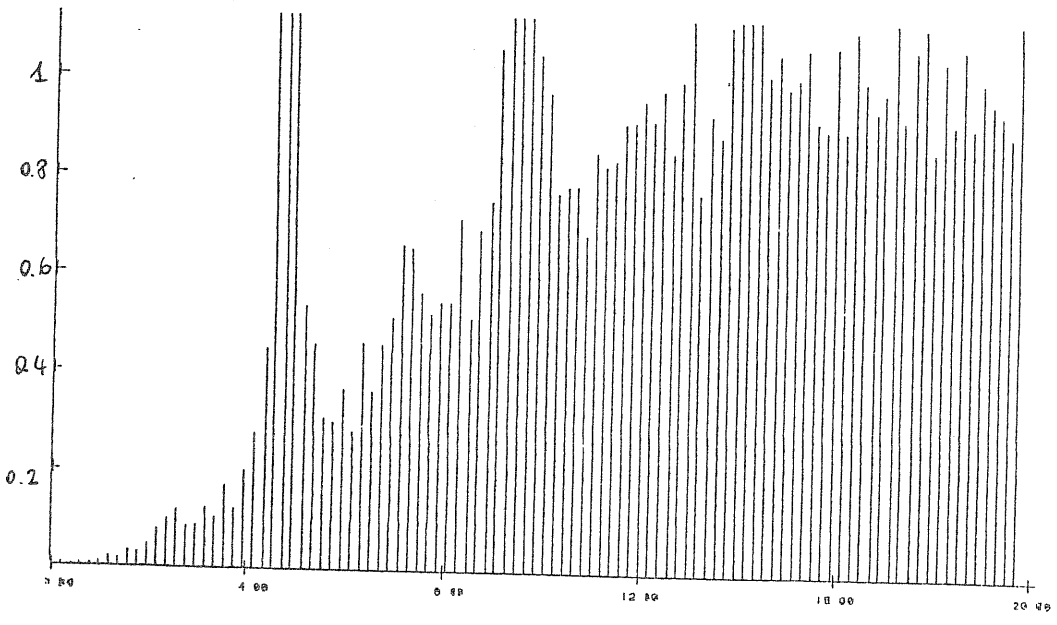

FIG. 25

T = 600 K

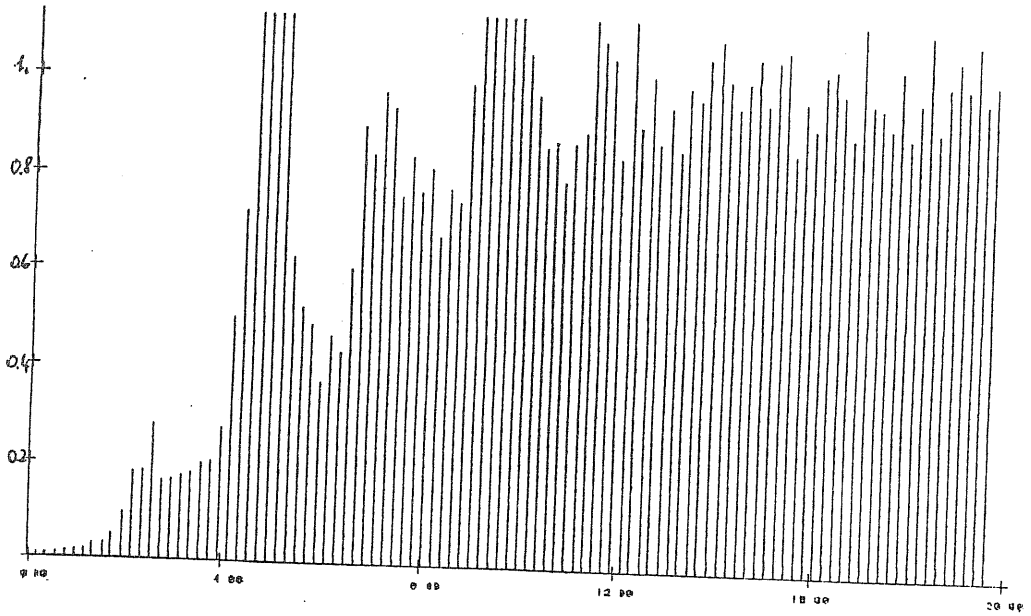

FIG. 26

T = 900 K

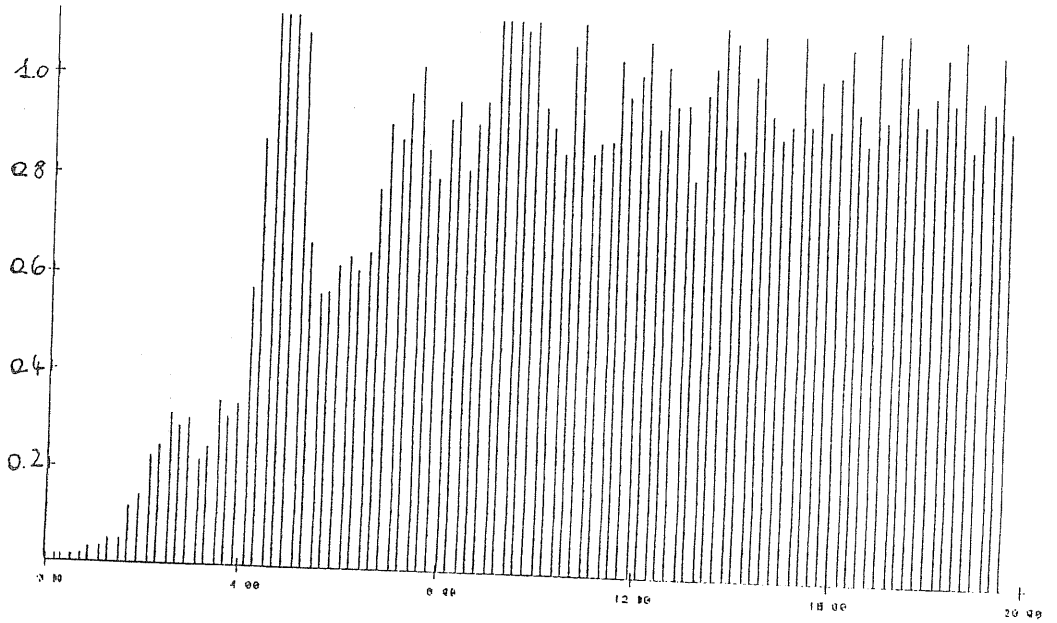

FIG. 27

T = 1200 K

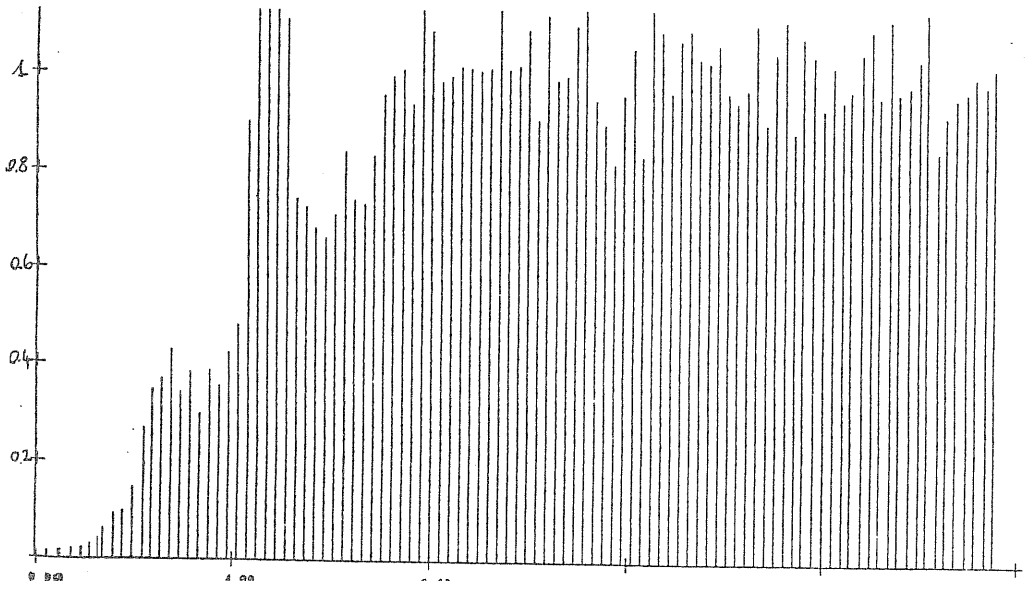

FIG. 28

T = 1400 K

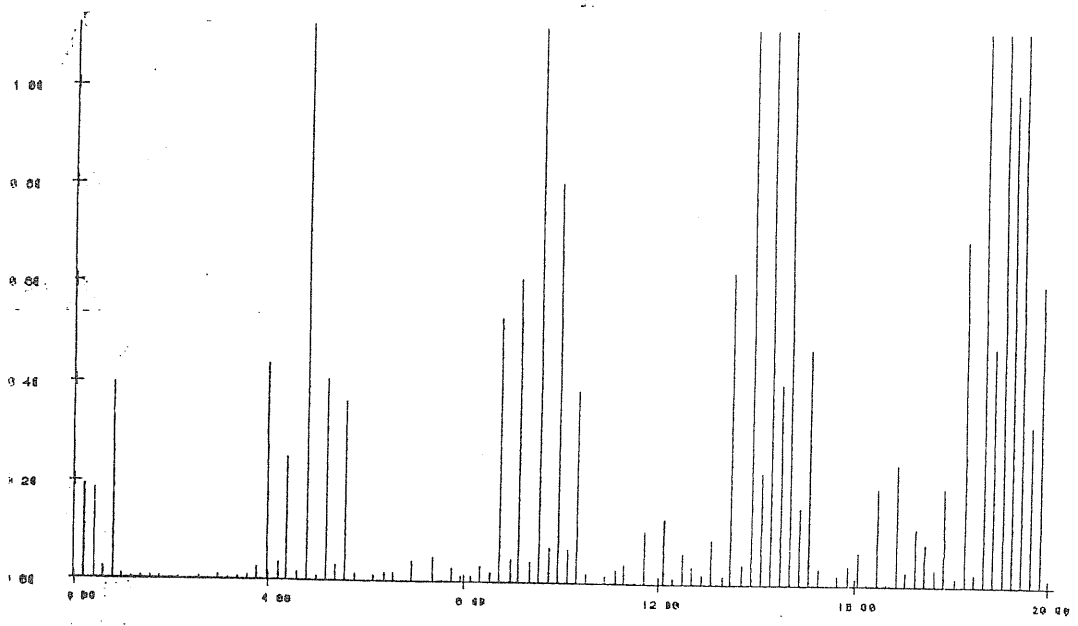

$S(K_x, K_z)$

FIG. 29

T=0

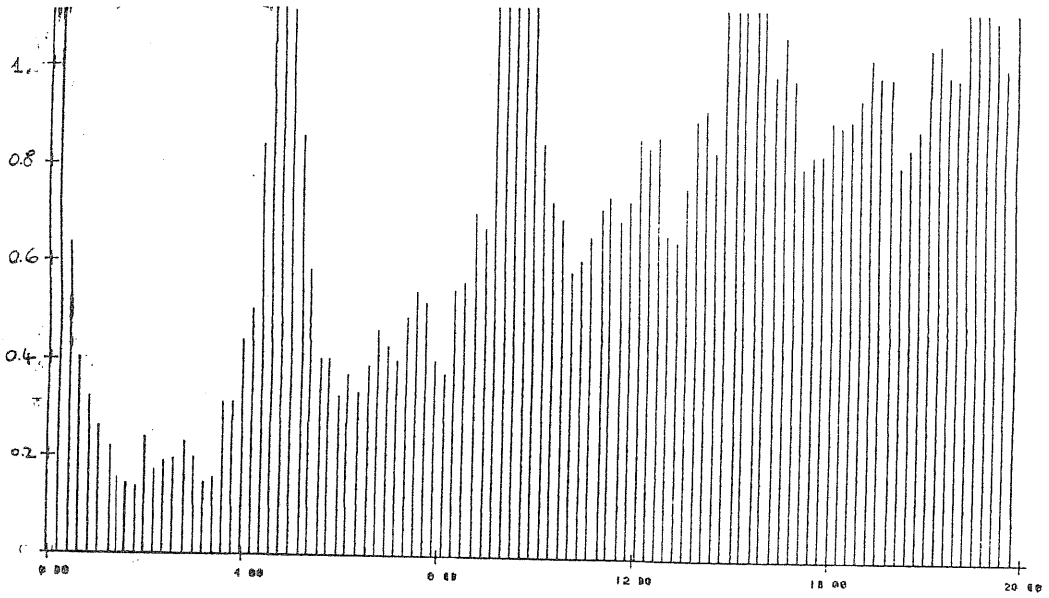

FIG. 30

T = 300 K

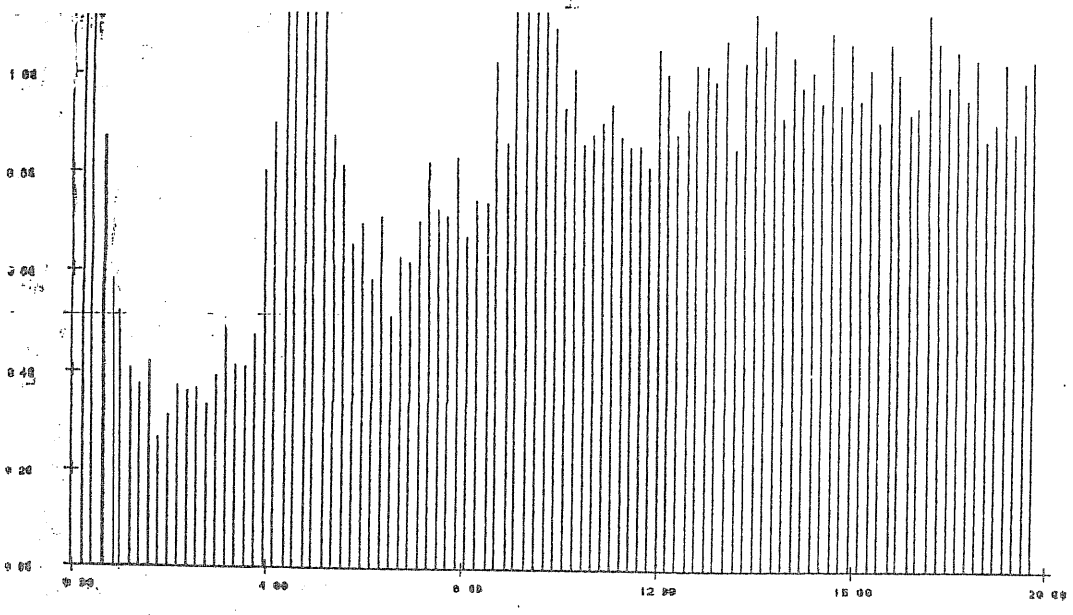

FIG.31

T= 600 K

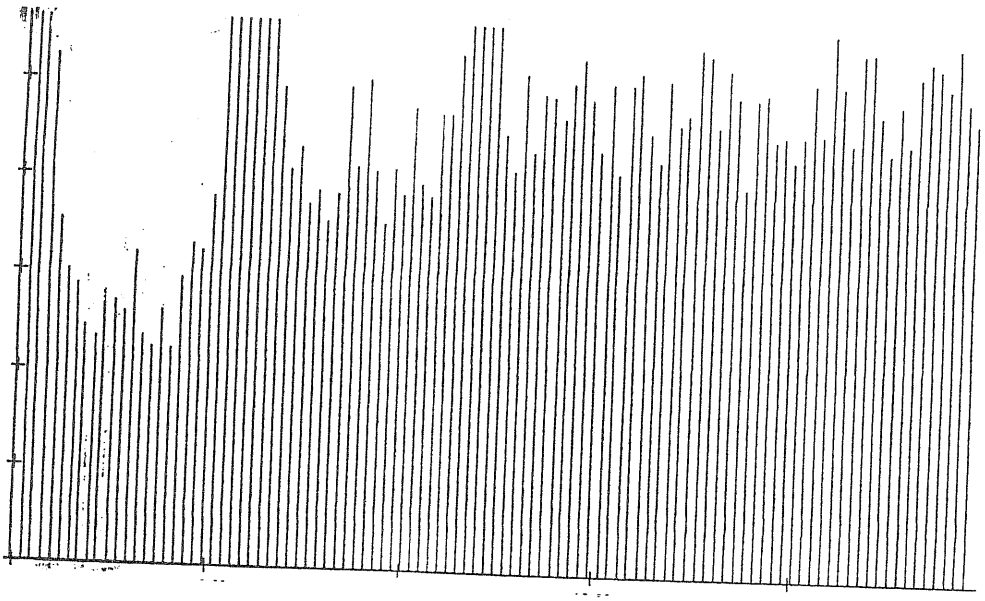

FIG. 32

T = 900 K

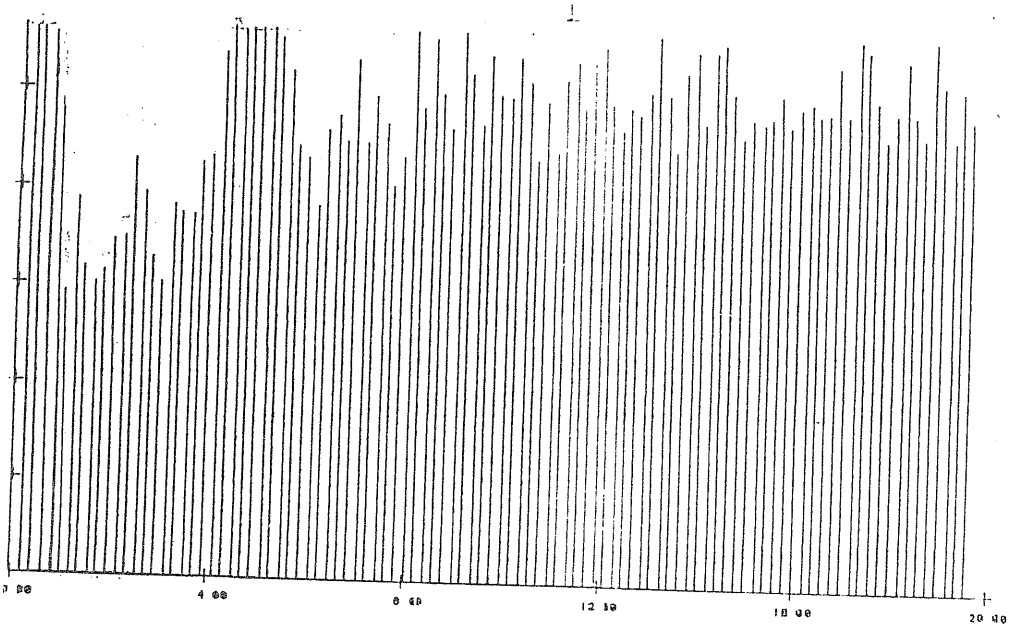

FIG.33

T = 1200 K

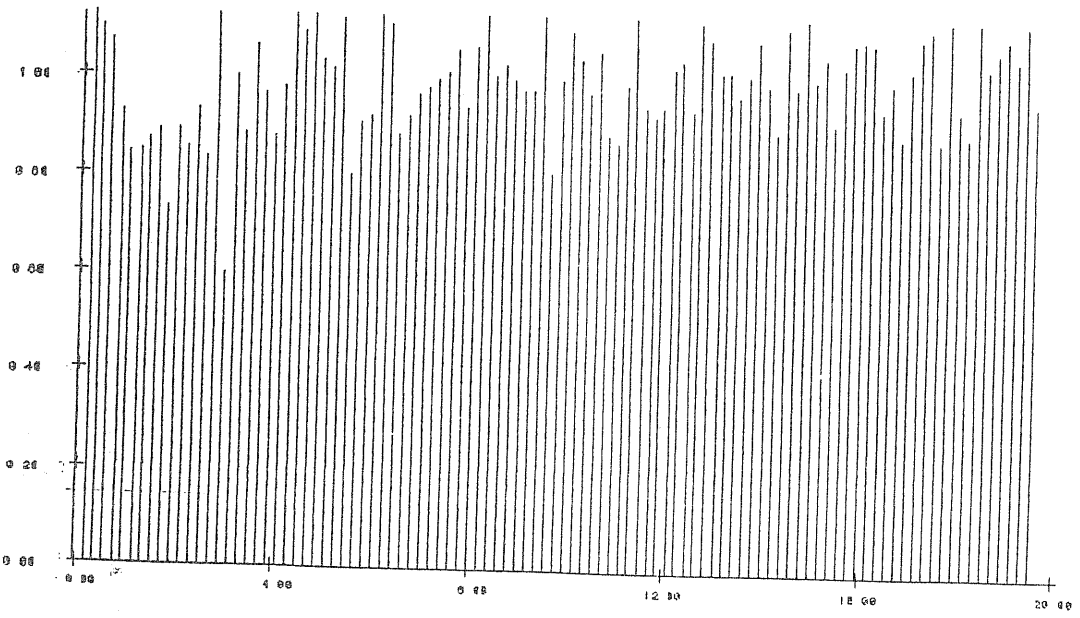

FIG.34

T = 1500 K

3.4 - Decay of phase correlations

We have seen that around 1400 °K the disorder starts to appear in the structure of the Au (111) surface, while at lower temperatures we can expect to be in a floating (incommensurate) phase.

This can be argued following the suggestion of what happens in W (001) surface (49), where the transition from order to disorder occurs through a sequence of narrow, but well defined intermediate phases.

For W (001) the nature of these phases, which are found to be incommensurate, is discovered by studying the surface spatial correlations $C(R_{lm}) = \langle \cos\varphi_l \ \cos\varphi_m \rangle$. For large separation R_{lm} a non-zero constant limit of $C(R_{lm})$ indicates long range order, an exponential decay indicates disorder, and a power law decay of $C(R_{lm})$ is expected for a two dimensional floating phase (appendix 1).

The phase (relative to (110) direction) which has been studied in W (001) is defined through the following formula:

$$\vec{R}_i(l) = \vec{R}^{\circ}_i(l) + \vec{\rho}\ e^{-\frac{la}{2\lambda}} \left(e^{i\vec{q}\vec{R}_i(l) + \pi l} + C.C. \right) \qquad (15)$$

$$\rho = |\vec{\rho}|$$

$$\varphi = \operatorname{tang}^{-1} \frac{\rho_x + \rho_y}{\rho_x - \rho_y} \qquad (16)$$

where ρ is the reconstruction order parameter, λ a penetration depth and $\vec{R}_i(l)$ the unperturbed position of atom i in layer l (l = 0 denoting the surface).

In the case of Au (111) we have taken, as our phase $\varphi_n = \frac{2\pi}{b}(x_n - nb)$ already used in our previous calculations (paragraph 3.2). We have just started the study of correlations with the definition of such a phase.

To have a rough idea of the trend of correlations, we have calculated them only at two temperatures, 1000 °K and 1500 °K.

For what concerns 1000 °K we thought that it could illustrate a range of temperature in which we could expect the presence of a floating (incommensurate) phase, so a power law decay of correlations.

At 1500 °K, instead, we expected to be in a completely disordered phase with exponential decay of correlations (19).

Therefore, in a graph with $\ln C(R_{lm})$ in function of R_{lm} we thought to get a linear shape in both cases. We thought to get a straight line with angular coefficient equal to 1/2. In fact the coefficient η for the power law decay of correlations ($\langle S(0)S(r)\rangle \sim r^{-\eta} \cos \vec{q}.\vec{r}$ in a floating phase is shown to be $\eta = 2/p^2$ by Schulz (26) with p linked to the number of domains separated by walls of solitons. In our case p = 2 for the presence of the regions fcc and hcp.

But the shape of the graphs has not resulted like we expected, but oscillating rapidly. As we expected, instead, we have seen that correlation decreases if the distance increases (figg. 35-36).

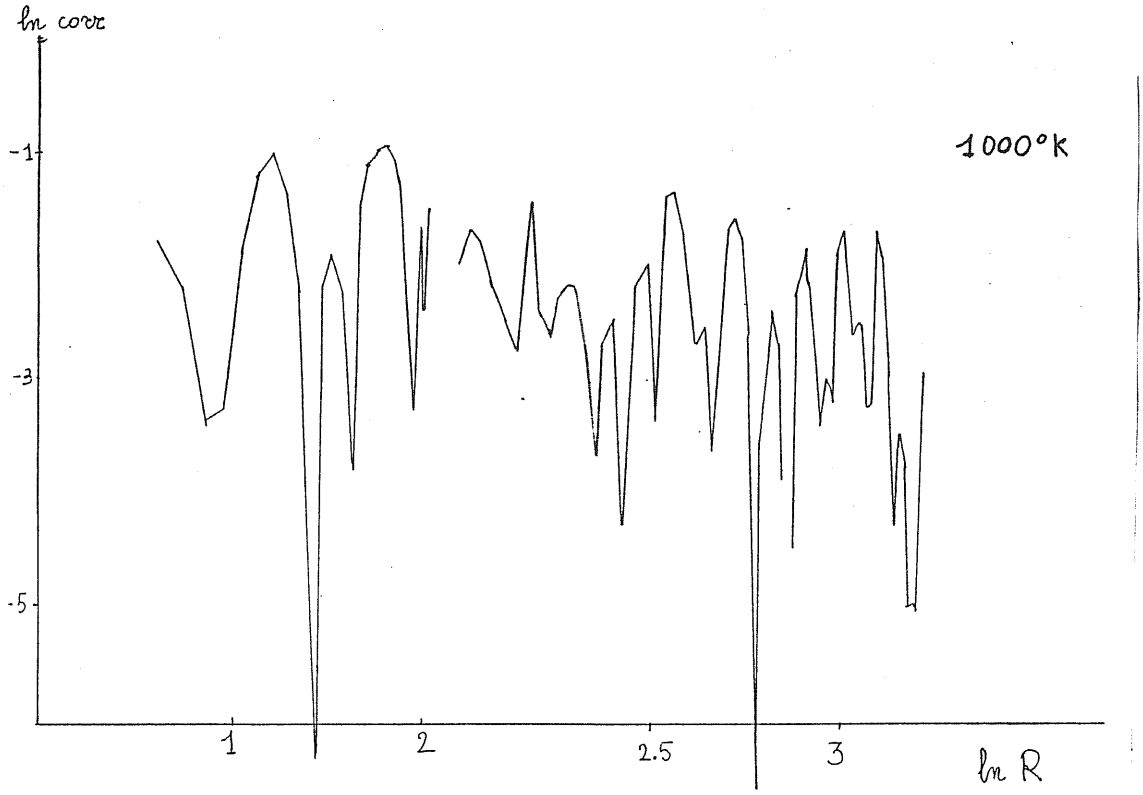

FIG. 35

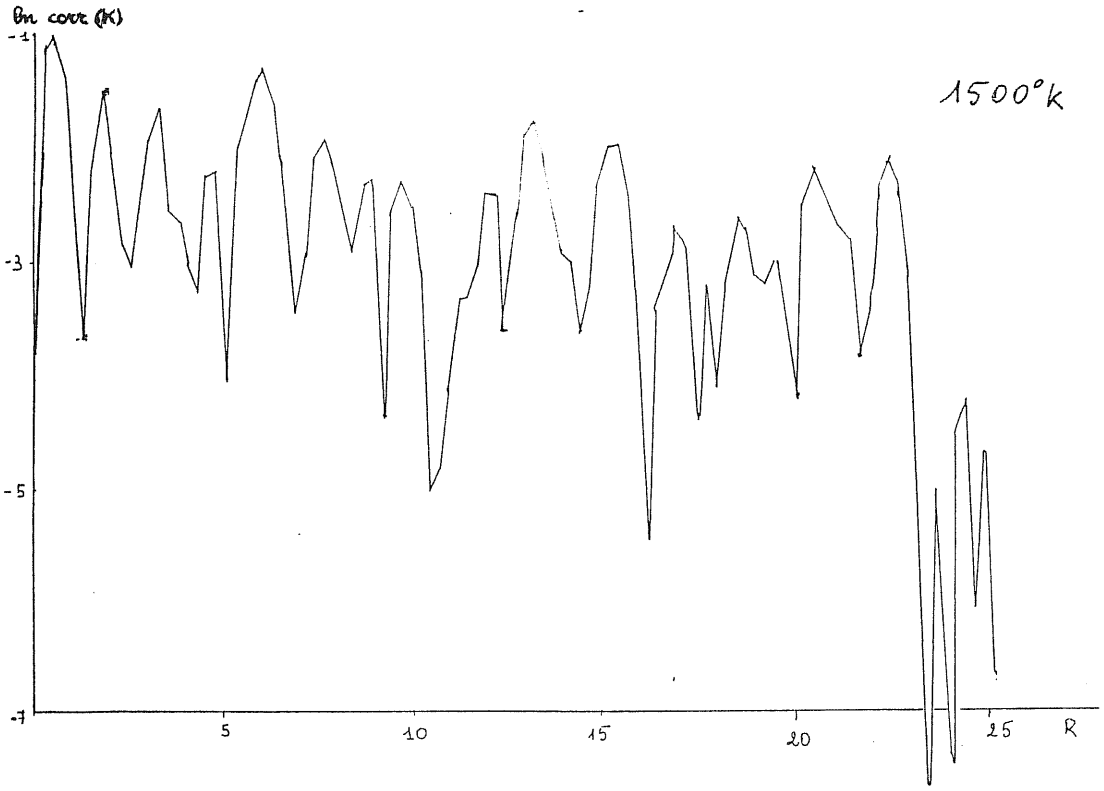

FIG. 36

CONCLUSIONS AND POSSIBLE OUTLOOKS

The first part of this thesis is a review about some models proposed to explain experimental data on Au (111) surface; after this review, we have studied the structure of this reconstructed surface using a phenomenological Hamiltonian, including a many body term, the "glue", determined in such a way to account for a large variety of properties of solid and liquid gold.

We have discussed the importance of this term, putting in evidence the inadequacy of a pairwise description for many properties of metals.

We have also described general approaches in which many body terms similar to the glue are considered.

The essential part of the research project described in this thesis is contained in section 3. Many of the results given there are tentative and often incomplete and , in fact,the study is continuing.

The optimal atomic configuration of Au (111) slabs is obtained by a molecular dynamics strategy at every temperature.

At T=0 the lowest energy configuration is found to be $(11x2\sqrt{3})$. We have explained that the structure at T=0 is characterized by domains in which the structure is fcc or hcp and the transition between the two regions is characterized by the presence of solitons.

We have studied also the changing in the structure rising

temperature and we have noted that that the reconstruction starts to disappear only at very high temperature (over 1400 °K, when the system is in a metastable state).

To observe in the detail the region of high temperature and the transition from a floating to a disordered phase, we have started the study of correlations, which show oscilllating behaviour both in the phase which should be incommensurate and in the disordered one.

To do a more detailed study of the Au (111) surface reconstruction with temperature we should investigate how the fcc and hcp regions and the solitons move at the various temperatures and in particular how many times the soliton walls oscillate in the period which the simulation lasts. To do this we should write a program that, at every time step, check which atoms are in bridge with the second layer and which are in fcc or hcp domains or, more simply, to study every 500 steps, for istance, the positions of the particles, to investigate their movements.

A further problem is linked to the choice of the right number of time steps. We have seen, in fact, that the system passes through metastable equilibrium states, before reaching a position of stable equilibrium which is obtainable only with a very large number of time steps.

The problem to get well equilibrated states is evident at every temperature, having seen to change the results, changing

the number of time steps. Perhaps the equilibration times for such system are really very long, it may be too long to be useful molecular dynamics.

In spite of these open problems, the progress made in understanding the Au (111) surface with this approach seems encouraging, and will be further pursued in the future.

A P P E N D I X 1

Here we shall shortly describe the theory of solitons (19) and Frenkel Kontorova model (20) in the solution of Frank and Van der Merwe (21).

The Hamiltonian of Frenkel Kontorova model is the following:

$$\mathcal{H} = \sum_n (x_{n+1} - x_n - a_o)^2 + V\left(1 - \cos\frac{2\pi}{b} x_n\right) \qquad (17)$$

An array of atoms connected with harmonic springs, interacts with a periodic potential of period b; a_o is the lattice constant which, in general, would be incommensurate with b. The model is a one dimensional zero temperature one.

In a diffraction experiment, one would observe Bragg spots at positions $Q = \frac{2\pi}{a} N$. None of these spots coincide with the Bragg spots of the periodic potential at positions $G = \frac{2\pi}{b} M$. But if the potential is strong enough, it may be favourable for the lattice to relax into a commensurate structure where the average lattice spacing a, is a simple rational fraction of the period b. The diffraction pattern of the substrate and the adsorbed layer have an infinite set of coinciding Bragg sheets.

Incommensurate structures generally show up in systems with competing periodicities. In a solid state system, one of the periods is that of the basic lattice. The other period may be that of another lattice, as in the Frank and Van der Merwe model. Rare gas monolayers

adsorbed on graphite constitute a two dimensional realization of this situation.

Another example is given by a reconstructed surface. A reconstructed surface, in fact, can be formed from the regular surface by applying a periodic lattice distortion. The two periodicities are evidently that of the regular surface and that of the distortion.

The ground state of the 1D model now described was found in 1949 by Frank and Van der Merwe with the extra assumption that the discrete index n can be treated as a continuous variable. Introducing the phase φ_n by the equation

$$x_n = nb + \frac{b}{2\pi}\varphi_n \qquad (18)$$

and transforming to the continuum limit

$$\varphi_n - \varphi_{n-1} = \frac{d\varphi}{dn}\,, \qquad (19)$$

the Hamiltonian becomes:

$$H = \int \left[\frac{1}{2}\left(\frac{d\varphi}{dn} - \delta\right)^2 + V\,(1-\cos p\varphi)\right] dn \qquad (20)$$

$p = 1$, $\delta = (a_o - b)\frac{2\pi}{b}$ is the natural misfit between the two lattices. With $p > 1$, H describes the transition to a commensurate phase of order p . The phase φ is the shift of the atoms relative to the potential minima. The state $\varphi(n) = 0$ is the commensurate phase, and the unperturbed incommensurate phase is given by the straight line $\varphi = \delta n$.

The ground state which minimizes the Hamiltonian is found

among the solutions to the 1D sine-Gordon equation

$$\frac{d^2\varphi}{dn^2} = pV \sin p\varphi \qquad (21)$$

One of the solutions to this equation is the soliton

$$\varphi(n) = \frac{4}{p}\tan^{-1}\exp(p\sqrt{V}\, n) \qquad (22)$$

The solution describes a wall, centered at $n = 0$ which separate two commensurate regions, one with $\varphi = 0$, the other with $\varphi = \frac{2\pi}{p}$.

The wall represents an extra atom which has been added to the chain within a region given by the soliton width $l_o = 1/p\ V$.

In general the solutions are regularly spaced solitons, a soliton lattice. The soliton lattice is a compromise between the "umklapp" term $\cos p\varphi$ which favours $\varphi = \frac{2\pi m}{p}$ and the elastic energy which favours $\varphi = \delta\ n$. The concept of walls, now introduced, plays a very central role in all existing theories of commensurate- incommensurate transitions (CI) (figg. 37-38).

The average misfit between the chain and the lattice $\bar{q} = \frac{2}{b}(a-b)$ is inversely proportional to the distance l between the domain walls $\bar{q} = 2\pi/pl$.

Near the commensurate phase, where the soliton density is low, the energy density takes the form

$$E = \left(\frac{4\sqrt{V}}{\pi} - \delta\right)\bar{q} + \frac{16\sqrt{V}}{\pi}\ \bar{q}\ \exp\left(-\frac{2\pi\sqrt{V}}{q}\right) \qquad (23)$$

The first term is proportional to the soliton density and may therefore be considered as the soliton energy.

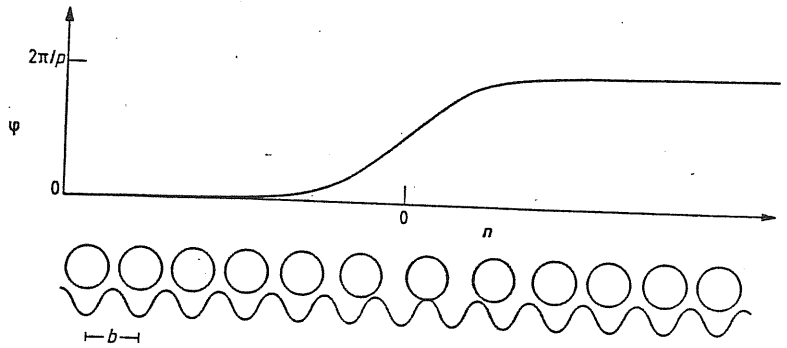

Figure 37 Single-soliton solution to the FVdM model. The soliton is a domain wall between two commensurate regions.

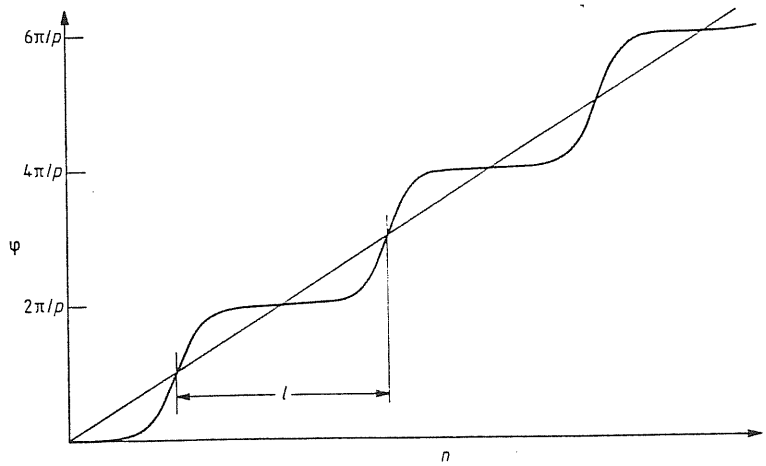

Figure 38 Regular soliton lattice solution to the sine-Gordon equation (2.4). The straight line corresponds to an unperturbed incommensurate structure.

The second term decays exponentially with the distance between solitons, and it is thus an effective repulsion between solitons. When V becomes small enough (or δ large enough) so that the soliton energy becomes negative, the C phase becomes unstable with respect to spontaneous formation of walls. This equation thus determines the CI transition.

We must say something also about CI transitions in two dimensions (19,22).

It can be shown that in two dimensions an incommensurate phase with long range order cannot exist. The incommensurate phase will be a "floating phase" with no long range order, but with an algebraic decay of correlations function. More precisely, the order parameter correlation functions take the following forms in the various C and I phases (q is the wavevector of the phase) at long distances

$$\begin{aligned}
&\text{a) incommensurate:} && \langle S(0)S(r)\rangle \sim \cos(\vec{q}\cdot\vec{r} + \varphi) \\
&\text{b) floating} && : \langle S(0)S(r)\rangle \sim r^{-\eta}\cos(\vec{q}\cdot\vec{r} + \varphi) \\
&\text{c) fluid} && : \langle S(0)S(r)\rangle \sim \exp(-\vec{k}\cdot\vec{r})\cos\vec{q}\cdot\vec{r} \qquad (24) \\
&\text{d) commensurate} && : \langle S(0)S(r)\rangle \sim \cos(\vec{q}_0\cdot\vec{r}),\ q_0 \text{ commensurate, locked}
\end{aligned}$$

It is important to remark that the floating phase with incommensurate wavevector and power law decay, is believed to exist only in two dimensions. The transition between the fluid and the floa-

ting phase is driven by dislocations or vortices, like in the Kosterlitz- Thouless (23-24) transition, instead the CI transition is triggered by an instability with respect to walls.

For the CI transitions it is important the theory of Pokrovsky and Talapov (25) which takes walls into account, but ignores vortices. A more general model, including also dislocations, has been given by Schulz (28).

The theory of Pokrovsky- Talapov applies to the CI transition in the case of one dimensional potential. In this model walls cross from one end of the sample to the other and are not allowed to cross or turn backwards.

The starting point is a generalization in two dimensions of the KVdM model

$$\mathcal{H} = \int \left[\frac{1}{2}\gamma\left(\frac{d\varphi}{dy}\right)^2 + \frac{1}{2}\left(\frac{d\varphi}{dx} - \delta\right)^2 + V \cos p\varphi \right] dx\, dy \qquad (25)$$

It should be shown that the calculation of the free energy of the 2D model amounts to the calculation of the ground state energy of the 1D quantum Hamiltonian H

$$\hat{H} = \int \left[C\pi^2 + \frac{1}{2}\left(\frac{d\varphi}{dx} - \delta\right)^2 + V \cos p\varphi \right] dx \qquad (26)$$

with C = 1/2. This is the 1D quantum sine Gordon equation with a soliton chemical potential δ .

In this model there is a phase transition when the quantum soliton energy equals the chemical potential. Pokrovsky and Talapov

found also an extra term to be added to the wall energy at non-zero temperature of the order $1/l^3$ which overwhelms the exponential term in formula (23) for large l. The $1/l^3$ term can be understood qualitatively on the basis of the wandering (or diffusion) of the walls.

Pokrovsky and Talapov found also the power law correlation functions characteristic of the floating phase.

Schulz (26) has solved a fermion version of equation (23) at a special temperature and his findings are in agreement with those of Pokrovsky and Talapov. Schulz also finds the exponent near the CI transition to be $\eta = 2/p^2$.

A P P E N D I X 2

The predictor-corrector type algorithm, which can be found in a report by Gear(47), makes use of the derivates of q up to a predeterminated order, say 5, for example, and all these derivates need to be carried in the memory. Let's denote q by q_0, $\dot{q}\Delta t$ by q_1, $\ddot{q}(\Delta t)^2/2!$ by q_2 and so on. The first step is to predict the values of all the derivates at $t + \Delta t$ using a Taylor expansion. At $t + \Delta t$ let p_i be the predicted values of q_i. We have

$$p_0 = q_0 + q_1 + q_2 + q_3 + q_4 + q_5$$

$$p_1 = q_1 + 2q_2 + 3q_3 + 4q_4 + 5q_5$$

$$p_2 = q_2 + 3q_3 + 6q_4 + 10q_5$$

$$p_3 = q_3 + 4q_4 + 10q_5$$

$$p_4 = q_4 + q_5$$

$$p_5 = q_5$$

Hence from p_2 we can get the predicted value of the acceleration at $t+\Delta t$. Using p_0 the predicted positions at $t + \Delta t$ we can calculate the accelerations in predicted positions; let $a(p_0)$ denote this value and let $\tilde{p}_2$ denote $a(p_0)(\Delta t)^2/2!$. It is the difference $\Delta = \tilde{p}_2 - p_2$ which allows us to get corrected values c_i for all the predicted values p_i as follows:

$$c_i = p_i + f_{i2}^{(5)} \qquad i = 0, 1, \ldots, 5$$

where the numbers $f_{i2}^{(5)}$ are 3/16, 251/360, 1, 11/18, 1/6, 1/60, respec-

tively for i = 0, 1 .....5. In $f_{ij}^{(k)}$, j denotes the order of the differential equation being solved, (k) the order of the highest derivative being used in the algorithm and i goes from 0 to k.

It is important to note that for clarity of presentation we have used the symbols p and c. In fact , the only memory locations needed are for the q's and for the acceleration $a(p_o)$ mentioned above.

The predictor-corrector method has the advantage that one can use the differences $c_o - p_o$ and $c_1 - p_1$ to put bounds on the acceptable error. The predictor- corrector loop can be repeated if necessary by using the corrected values as the predicted values and going back to the calculation of $a(c_o)$ and then Δ would be $\tilde{c}_2 - c_2$, $\tilde{c}_2$ being $a(c_o) \times (\Delta t)^2/2!$.

This algorithm has other possibilities too; it allows us to solve a coupled set of 1st and 2nd order differential equations in the same manner as explained above. As for the problem of initiating the calculation, a practical scheme would be to put all the derivates from 2 upwards equal to zero; in a few steps of Δt the algorithm itself generates appropriate values. More sophisticated methods of starting a calculation can also be used but in the contest of statistical mechanics the error committed in the first few Δt has no significance at all for the final results stretching over thousands of Δt.

REFERENCES

(1) M.A. Van Hove, R.J. Koestner, P.C. Stair, J.P. Biberian, L.L. Kesmodel, I. Bartos and G.A. Somorjai, Surf. Science 103 , 189 (1981)

(2) M.A. Van Hove, R.J. Koestner, P.C. Stair, J.P. Biberian, L.L. Kesmodel, I. Bartos and G.A. Somorjai, Surf. Science 103, 218 (1981)

(3) D.G. Fedak, N.A. Gjostein, Acta Met. 15, 827 (1967)

(4) D.G. Fedak, N.A. Gjostein, Surf. Science 8, 77 (1967)

(5) D.G. Fedak, N.A. Gjostein, Phys. Rev. Lett. 16, 171 (1966)

(6) M. Kostelitz, J.L. Damange, J. Oudar, Surf. Science 34 , 431 (1973)

(7) M.A. Chesters, G.A. Somorjai, Surf. Science 52, 21 (1975)

(8) J. Perdereau, J.P. Biberian, G.E. Rhead, J. Phys. F 4, 798 (1974)

(9) D.M. Zehner, J.F. Wendelken in Proc. 7th Intern. Vacuum Congress and 3rd Intern. Conf. on Solid Surfaces, Vienna (1977)

(10) H. Melle, E. Menzel, Z. Naturforsh 33a, 282 (1978)

(11) K. Yagi, K. Takayanagi, K. Kobayashi, N. Osakabe, Y. Tanishiro, G. Honjo, Proc. 9th Intern. Cong. on Elec.Microscopy, Toronto (1978)

(12) K. Yagi, K. Kobayashi, N. Osakabe, Y. Tanishiro, G. Honjo, Surf. Science 86, 174 (1979)

(13) J.C. Heyraud, J.J. Metois,Surf. Science 100, 519 (1980)

(14) Y. Tanishiro, H. Kanamori, K. Takayanagi, K. Yagi, G. Honjo, Surf. Science 111, 395 (1981)

(15) K. Takayanagi, K. Yagi, Trans. Jpn. Inst. Met. 24, 337 (1983)

(16) L.D. Marks, V. Heine, D.J. Smith, Phys. Rev. Lett. 52, 656 (1984)

(17) V. Heine, L. D. Marks, Surf. Science 165, 65 (1986)

(18) U. Harten, A.M. Lahee, J.P. Toennies, C.H. Woll, Phys. Rev. Lett. 54, 2619 (1985)

(19) P. Bak, Reports on Progress in Physics, 589 (1982)

(20) Y.I. Frenkel, T. Kontorova, Zh. Eksp. Teor. Fiz. 8, 1340 (1938)

(21) F.G.Frank, J.W. Van der Merwe, Proc. R. Soc. London 198, 205 (1949)

(22)R.F. Willis in Dynamical Phenomena at Surfaces, Interfaces and Superlattices ed. by F. Nizzoli, K.H. Rieder, R.F. Willis, Springer Verlag

(23) J.M. Kosterlitz, J. Phys. C 7 ,1046 (1974)

(24) J.M. Kosterlitz, D.J. Thouless, J. Phys. C 6, 1181 (1973)

(25) V.L. Pokrovsky, A.L. Talapov, Zh. Eksp. Teor. Fiz. 75, 1151 (1978)

(26) H.J. Schulz, Phys. Rev. B 22, 5274 (1980)

(27) T. Engel and K.H. Rieder in "Structural Studies of Surfaces" ed. by I. Strell and G. Schudt Weitz Springer Tracts in Modern Physics, vol. 91 , Springer Verlag

(28) H.J. Schulz, Phys. Rev. B 28, 2746 (1983)

(29) L.D. Marks, D.J. Smith,Surf. Science 143, 495 (1985)

(30) F. Jona,J. Phys. C 11, 4271 (1978)

(31) J. Friedel, Ann. Phys. (Paris) 1, 257 (1976)

(32) R.P. Gupta, Phys. Rev. B 23, 6265 (1981)

(33 M.S.Daw, M.I. Baskes,Phys. Rev. Lett. 50, 1285 (1983)

(34) M.S.Daw, M.I. Baskes,Phys. Rev. B 29, 6443 (1984)

(35) S.M. Foiles, M.S. Daw, M. I. Baskes, Phys. Rev. B 33, 7983 (1986)

(36) B.M. Finnis, J.E. Sinclair, Phyl. Mag. A 50, 45 (1984)

(37) F. Ercolessi, E. Tosatti, M. Parrinello, Phys. Rev. Lett. 57 , 719 (1986)

(38) R.A. Johnson, Phys. Rev.B 6, 2094 (1972)

(39) M.J. Stott, E. Zaremba, Phys. Rev. B 22, 1564 (1980)

(40) P. Hohemberg, W. Kohn, Phys. Rev.B 136, 864 (1964)

(41) F. Ercolessi, Magister Thesis (1986) - SISSA

(42) F. Ercolessi, M. Parrinello, E. Tosatti, to be published

(43) M. Garofalo, E. Tosatti, F. Ercolessi, to be published

(44) M. Garofalo, Magister Thesis (1984) - SISSA

(45) A. Rahman, Phys. Rev. 136 A, 405 (1964)

(46) A. Rahman, in NATO Advanced Studies Institute Series (1977)

(47) C. W. Gear, ANL Report 7126, Argonne National Laboratory and Numerical Initial Value Problems in Ordinary Differential Equations (Pretice Hall, Englewood Cliffs, N. J. 1971)

(48) P. Carnevali, F. Ercolessi, E. Tosatti, private communication

(49) C. Z. Wang, M. Parrinello, E. Tosatti, A. Fasolino, to be published